Chromatin-remodeling factor OsINO80 is involved in regulation of gibberellin biosynthesis and is crucial for rice plant growth and development

Chao Li, Yuhao Liu, Wen-Hui Shen, Yu Yu, Aiwu Dong

Chromatin-remodeling factor OsINO80 is involved in regulation of gibberellin biosynthesis and is crucial for rice plant growth and development

Chao Li[1], Yuhao Liu[1], Wen-Hui Shen[1,2], Yu Yu[1,*], and Aiwu Dong[1,*]

[1] State Key Laboratory of Genetic Engineering, Collaborative Innovation Center of Genetics and Development, Institute of Plant Biology, School of Life Sciences, Fudan University, Shanghai 200433, China

[2] Institut de Biologie Moléculaire des Plantes, UPR2357 CNRS, Université de Strasbourg, 12 rue du Général Zimmer, 67084 Strasbourg Cédex, France

*Correspondences: aiwudong@fudan.edu.cn (Dr. Aiwu Dong is fully responsible for distributions of all materials associated with this article); yuy@fudan.edu.cn

Running title: OsINO80 promotes GA biosynthesis

Abstract

The phytohormone gibberellin (GA) plays essential roles in plant growth and development. Here, we report that OsINO80, a conserved ATP-dependent chromatin-remodeling factor in rice (*Oryza sativa*), functions in diverse biological processes and GA biosynthesis. *OsINO80*-knockdown mutants, derived from either T-DNA insertion or RNA interference, display typical GA-deficient phenotypes, including dwarfism, reduced cell length, late flowering, retarded seed germination and impaired reproductive development. Consistently, transcriptome analyses reveal that *OsINO80* knockdown results in down-regulation by more than two-fold of over 1000 genes, including the GA biosynthesis genes *CPS1* and *GA3ox2*, and the dwarf phenotype of *OsINO80*-knockdown mutants can be rescued by the application of exogenous GA3. Chromatin immunoprecipitation (ChIP) experiments show that OsINO80 directly binds to the chromatin of *CPS1* and *GA3ox2* loci. Biochemical assays prove that OsINO80 specially interacts with histone variant H2A.Z and the H2A.Z enrichments at *CPS1* and *GA3ox2* is decreased in *OsINO80*-knockdown mutants. Thus, our study identified a new rice chromatin-remodeling factor, OsINO80, and demonstrated that OsINO80 is involved in regulation of the GA biosynthesis pathway and plays critical functions at many aspects of rice plant growth and development.

Keywords: rice; gibberellin, chromatin-remodeling factor, transcriptional regulation

INTRODUCTION

Gibberellins (GAs) are important endogenous phytohormones and modulate diverse plant developmental processes, including seed germination, leaf and stem elongation, flowering transition, and reproductive development (Hedden and Sponsel 2015). By searching for GA-deficient mutants, the key components in the GA pathway, including seven types of enzymes responsible for GA biosynthesis and metabolism, have been identified from both *Arabidopsis thaliana* and rice. The enzymes comprise ent-copalyl diphosphate synthase (CPS), ent-kaurene synthase (KS), ent-kaurene oxidase (KO), ent-kaurenoic acid oxidase (KAO), GA 20-oxidase (GA20ox), GA 3-oxidase (GA3ox), and GA 2-oxidase (GA2ox) (Sakamoto 2004; Sun 2008). In addition, knowledge has also been gained on some important regulators mediating GA signal transduction. It is known that GIBBERELLIN INSENSITIVE DWARF1 (GID1) proteins act as GA receptors, while Arabidopsis DELLA and rice SLENDER RICE1 (SLR1) are negative regulators of GA signaling (Ueguchi-Tanaka et al. 2007). Dwarfism is the typical phenotype of mutants defective in GA synthesis or signaling. In addition, GA-deficient plants often exhibit dark-green leaves, retarded growth, late flowering, and sterility (Sakamoto 2004; Sun 2008).

GA biosynthesis and signaling pathways allow plants rapidly responding to environmental changes, such as light, temperature, biotic and abiotic stresses (Yamaguchi 2008). Thus, GA-related genes tend to be precisely regulated during plant growth and development (Yamaguchi 2008). In recent years, several studies in Arabidopsis point to a link between the GA pathway and the chromatin-remodeling regulatory mechanism. There are four types of chromatin-remodeling factors in eukaryotes, the Swi/Snf, Iswi, Chd, and Ino80 families (Clapier and Cairns 2009). BRAHMA (BRM), the ATPase subunit of Swi/Snf-type chromatin-remodeling complexes, is a positive regulator of GA-mediated responses in Arabidopsis (Archacki et al. 2013). SWI3C, a core component of the Arabidopsis Swi/Snf-type chromatin-remodeling complexes, physically interacts with DELLA proteins, and this interaction is necessary for proper GA biosynthesis and signaling (Sarnowska et al. 2013). The Chd-type chromatin-remodeling factor PICKLE (PKL) also interacts with DELLA proteins and functions in Arabidopsis GA-dependent responses (Henderson 2004; Zhang et al. 2014). The Iswi-type CHROMATIN REMODELING 11 (CHR11) and CHR17 have been shown to be involved in Arabidopsis flowering transition, reproductive development, and genome-wide nucleosome

distribution (Huanca-Mamani et al. 2005; Li et al. 2012; Li et al. 2014), and the Ino80-family members PHOTOPERIOD-INDEPENDENT EARLY-FLOWERING 1 (PIE1) and AtINO80 have been reported to play crucial roles in Arabidopsis genome stability and plant development (Noh and Amasino 2003; Fritsch et al. 2004; Choi et al. 2007; Rosa et al. 2013; Zhang et al. 2015). Yet, whether or not Arabidopsis CHR11/CHR17 and PIE/AtINO80 also participate in GA-related process remains currently unknown.

So far, only a few chromatin-remodeling factors have been reported in rice (*Oryza sativa*). OsCHR4, a rice Chd-type chromatin-remodeling factor, was shown to be required for chloroplast development in the adaxial mesophyll (Zhao et al. 2012). CHR729, the rice homolog of PKL, was found to recognize methylated histone H3 lysine 4 (H3K4) and H3K27 and affect many aspects of plant development (Hu et al. 2012). Thus, it is important to characterize more rice chromatin-remodeling factors to uncover their biological functions.

In this study, we demonstrate that *OsINO80*-knockdown mutants display typical GA-deficient phenotypes and reduced levels of endogenous GAs. It is found that OsINO80 regulates GA biosynthesis by directly binding chromatin at the GA biosynthesis genes *CPS1* and *GA3ox2*. Our data further showed that OsINO80 interacts with H2A.Z and that loss of OsINO80 affects H2A.Z enrichment at these GA biosynthesis genes. Taken together, our study unravels important function of OsINO80 and provides a first link between chromatin-remodeling mechanism and GA biosynthesis regulatory pathway in the agronomic important crop rice.

RESULTS

Heterozygous *osino80/+* mutant plants show a dwarf and late flowering phenotype

OsINO80 contains a long insertion embedded in the ATPase domain, which is the defining feature of Ino80-type distinct from other types of chromatin-remodeling factors (Figure S1A). Both quantitative reverse transcription (qRT)-PCR analysis using RNA extracted from different rice tissues (Figure S1B) and histochemical GUS staining analysis using the reporter $P_{OsINO80}$*::GUS* transgenic plants (Figure S1C) indicated that *OsINO80* is ubiquitously expressed in various rice tissues.

To explore the role of OsINO80 in plant development, a T-DNA insertion mutant of *OsINO80* (line PFG_1C-03165.R) was purchased from the database of T-DNA insertion mutant

populations (Yi and An 2013). This mutant was generated from the japonica-type cultivar ‘Hwayoung’ and has a T-DNA insertion in the first intron of the *OsINO80* gene (Figure 1A). We then performed backcrossing with the wild-type ‘Hwayoung’ for three generations to clean the mutant background. Using the hygromycin resistance gene embedded in the T-DNA insertion as the probe, we further performed Southern blotting to determine the T-DNA copy number in the mutant genome. When the genomic DNA of the heterozygous *OsINO80* T-DNA insertion mutant (hereafter *osino80/+*) was digested with either the restriction enzyme *Eco*RV or *Hind*III, a single band was observed (Figure 1B), indicating that *osino80/+* contains one T-DNA insertion.

Our PCR-based genotyping of 488 segregating plants from the self-pollinated *osino80/+* failed to identify any homozygous mutant plants (Figure 1C). In contrast to the 1:2 segregation ratio as expected for an embryonic/zygotic lethal mutation, a segregation ratio of approximately 1:1 was observed for the wild-type ‘Hwayoung’ compared to *osino80/+* ratio (Figure 1D), implying that not only embryonic lethal but also reduced gametophytic transmission has occurred in the mutant. Interestingly, the transcript level of *OsINO80* was reduced to nearly half in *osino80/+* (Figure 1E), and the heterozygous *osino80/+* plants showed obvious morphological abnormalities as compared with the wild-type ‘Hwayoung’ (Figure 1F). The heterozygous *osino80/+* plants are obviously dwarf at either the three-leaf (Figure S2A) or the heading developmental stage (Figure 1F). The panicle length of *osino80/+* is shorter, and internode length is reduced as compared with that of wild-type (Figure 1G, Figure S2B and S2C). The dwarf phenotype of the heterozygotes *osino80/+* may be caused by reduced cell elongation, because the cell length is obviously reduced in the second leaf sheath in the heterozygous mutant plants (Figure 1H and Figure S2D). Moreover, the *osino80/+* mutants showed a late-flowering phenotype when grown side by side at two locations with different latitudes, Shanghai with long-day (LD) conditions, and Sanya with short-day (SD) conditions. Under both conditions, the average heading dates of *osino80/+* were later than those of the wild-type plants. Only the data under LD conditions are shown in Figure 1I.

OsINO80 is involved in pollen germination and pollen tube elongation

To further investigate the function of *OsINO80* in reproductive development, we introduced an

enhanced yellow fluorescent protein (*YFP*)-tagged *OsINO80* construct driven by the maize Ubiquitin promoter (*P_{UBI}::OsINO80-YFP*) into the *osino80/+* plants. Using the PCR-based genotyping of progeny of self-pollinated transgenic plants (*P_{UBI}::OsINO80-YFP/osino80/+*), transgenic lines over-expressing *OsINO80-YFP* in the homozygous *osino80-/-* background *(P_{UBI}::OsINO80-YFP/osino80-/-)* (Figure S3A) were obtained, confirming that the homozygote lethality is indeed caused by a loss-of-function of *OsINO80.* Moreover, the transformation of *P_{UBI}::OsINO80-YFP* into homozygous *osino80-/-* partially rescued the physiological phenotypes shown in heterozygous *osino80/+* (Figure S3B), indicating that YFP-tagged OsINO80 protein is functional *in planta*. We then performed the reciprocal cross-based analysis between *osino80/+* and the wild-type 'Hwayoung' as shown in Table 1. The observed segregation ratio of F1 progeny was close to 1:1 according to the χ^2-test when *osino80/+* plant was used as a female. Conversely, when male *osino80/+* plants served as pollen donors, the segregation ratio was 0.175:1, critically deviated from 1:1. It indicates that loss of *OsINO80* mainly impairs male gametophyte development.

Because the *osino80/+* mutant plants develop normal flowers with normal pistils and stamens, pollen development was analyzed using cytological observations. The viable pollen grains were stained dark by I_2-KI solution, while the sterile grains were stained yellow or light red (Chhun et al. 2007). As shown in Figure 2A, the pollen viability in *osino80/+* is similar to that in wild-type 'Hwayoung'. No abnormities in the cell architecture of pollen grains between *osino80/+* and wild-type 'Hwayoung' were found using 4',6-diamidino-2-phenylindole staining (Figure 2B). Next, we performed *in vitro* pollen germination assays. In wild-type 'Hwayoung', 93% of pollen grains germinated and elongated, while only 55% of those from *osino80/+* plants germinated under the same conditions (Figure 2C and 2D), suggesting that the defect of *osino80/+* in reproductive development may be related to impaired pollen germination and pollen tube elongation.

RNA interference (RNAi) of *OsINO80* plants display similar phenotypes as *osino80/+*

To further verify the role of *OsINO80* in rice growth and development, we used an RNAi approach to knock down *OsINO80* expression in rice. The nucleotides 2,038 to 2,239 and 4,849 to 5,234 of the *OsINO80* transcript were selected to form the inverted repeats of a hairpin

structure driven by the cauliflower mosaic virus 35S promoter, and the two constructs were named *P_{35S}::OsINO80-RNAi-1* and *P_{35S}::OsINO80-RNAi-2*, respectively. *P_{35S}::OsINO80-RNAi-1* and *P_{35S}::OsINO80-RNAi-2* were transformed into the japonica-type cultivar Nipponbare to obtain the transgenic plants *osino80Ri-1* and *osino80Ri-2*, respectively. After four generations, 10 independent *osino80Ri-1* lines and 7 independent *osino80Ri-2* lines were obtained. As expected, *osino80Ri-1* and *osino80Ri-2* plants displayed dwarf phenotypes similar to that of the T-DNA insertion mutant *osino80/+*. In correlation with their *OsINO80* expression levels, *osino80Ri-1* plants showed less severe phenotypes than those of *osino80Ri-2* (Figure 3A and 3B). The lengths of the panicles and internodes of the *osino80Ri-1* and *osino80Ri-2* plants were shorter than those of the wild-type 'Nipponbare' plants at the mature stage (Figure S4A-S4C), and the 1,000-grain weight was also reduced in the RNAi mutants (Figure S4D). Moreover, we also observed a retardation in seed germination, a defect in pollen germination and a late-flowering phenotype in *osino80Ri-2* plants (Figure S4E-S4G). Using *osino80Ri-2* plants, which exhibited a more severe phenotype, we find that the decrease of plant height was probably caused by shorter cell length (Figure S4H and S4I).

OsINO80 modulates the transcription of a large number of genes involved in multiple processes, including GA-related genes

We then performed RNA sequencing (RNA-seq) to analyze global gene expression changes in *osino80Ri-2* plants. By analyzing two independent biological replicates, 1,269 genes were down-regulated and 728 genes were up-regulated more than twofold in *osino80Ri-2*, compared with the wild-type rice (Table S1). Furthermore, a gene ontology (GO) analysis revealed that OsINO80 modulates many genes involved in a broad range of biological processes (Figure 3C and 3D). Both the down- and up-regulated genes in *osino80Ri-2* enriched in functions related to stress response, including biotic stimuli, for example fungi as well as abiotic stimuli, such as oxidative stress, wounding, cold, and water deprivation (Figure 3C and 3D). Thus, our transcriptome analysis indicates that OsINO80 is required for normal expression of a large number of genes playing wide range of roles during plant growth and development.

OsINO80-knockdown mutants, derived from either T-DNA insertions or RNA interference, display typical GA deficient phenotypes such as delay of seed germination, plant body

dwarfism, cell length reduction, late flowering, and reproductive defects. This prompts us to check the transcription levels of GA-related genes in *osino80Ri-2* using the RNA-seq data. Consistently, the transcription levels of the GA synthesis genes *CPS1* and *GA3ox2* were down-regulated nearly 50% in *osino80Ri-2* as compared to wild-type, albeit the transcription levels of GA signaling genes *OsSLR1*, *OsGID1*, and *OsGID2* were not significantly changed (Table S2). Detail RNA-seq maps were shown for the down-regulation of *OsINO80*, *CPS1* and *GA3ox2* (Figure 3E-3G), and for the unchanged control gene *OsGID1* (Figure 3H) in *osino80Ri-2* compared with those in the wild-type plants.

OsINO80 is required for GA biosynthesis

To validate the mis-regulation of GA-related genes from the RNA-seq data, we analyzed the transcriptional levels of the GA-related genes by qRT-PCR assays in *OsINO80*-knockdown mutants and wild-type rice shoots. The examined genes include *CPS1*, *KS1*, *KO2*, *KAO*, *GA20ox2*, *GA3ox2*, and *GA2ox1*, which encode various enzymes involved in GA biosynthesis, and *OsSLR1*, *OsGID1* and *OsGID2*, which are involved in GA signaling pathways. The transcriptional levels of the GA signaling genes *OsSLR1*, *OsGID1*, and *OsGID2* were not obviously changed in *osino80Ri-2* compared with those in the wild-type plants (Figure 4A). Similar to the RNA-seq data, the genes *CPS1* and *GA3ox2*, which are responsible for the synthesis of bioactive GA, were down-regulated in the *osino80Ri-2* mutants compared to the wild-type plants, while the gene *KAO*, encoding an enzyme catalyzing the oxidation of ent-kaurenoic acid, was up-regulated (Figure 4A). The T-DNA insertion mutant *osino80/+* resembled the *OsINO80* RNAi mutants showing similar differential gene expression as analyzed using both rice shoots and anthers (Figure S5A and S5B), demonstrating that OsINO80 is required for GA biosynthesis through the modulation of genes encoding the key enzymes in the GA biosynthesis pathway. Moreover, the transformation of P_{UBI}*::OsINO80-YFP* into the homozygous *osino80-/-* rescued the GA-related gene mis-expression defects (Figure S5C).

We then examined the endogenous GAs in *osino80Ri-2* and the wild-type plants. The levels of GA_{12}, GA_{53}, GA_{19}, GA_{20} and GA_1 were decreased in *osino80Ri-2* compared with those in the wild-type rice (Figure 4B), validating a defect in GA biosynthesis in the *OsINO80*-knockdown

mutants. To further verify the defects of *osino80Ri-2* in GA biosynthesis, we performed an exogenous GA-treatment assay to check the responsiveness of *osino80Ri-2*. The plants were cultivated in Murashige and Skoog solid medium containing 0, 10^{-10}, 10^{-8}, 10^{-6}, or 10^{-4} M of the bioactive GA_3, and the length of the second leaf sheath was measured after 1 week. When the wild-type plants were treated with increasing concentrations of GA_3, the length of the leaf sheath increased. For *osino80Ri-2*, the leaf sheath length also increased with treatments of increasing GA_3 concentrations, and its dwarf phenotype was fully rescued at 10^{-4} M (Figure 4C). Similarly, the application of exogenous GA_3 also rescued the dwarf phenotype of the T-DNA insertion mutant *osino80/+* at 10^{-4} M (Figure S5D). All these data point to an important function of *OsINO80* in regulation of the GA biosynthesis pathway.

OsINO80 directly targets to the GA biosynthesis genes *CPS1* and *GA3ox2*

To analyze the function of OsINO80 protein *in planta*, we obtained transgenic plants over-expressing *OsINO80-YFP* driven by the maize Ubiquitin promoter (P_{UBI}*::OsINO80-YFP*) in the wild-type 'Nipponbare' background. The *OsINO80-YFP* transgenic plants showed an overexpression of *OsINO80* (Figure S6A), but no disturbance to GA-related genes' expression (Figure S6B). By observing the root apical cells of P_{UBI}*::OsINO80-YFP* transgenic plants, we determined that, consistent with its chromatin-related function, the OsINO80-YFP protein was localized in the nucleus (Figure 5A).

Using the transgenic plants, we examined the enrichment of OsINO80 at the GA biosynthesis genes *CPS1*, *GA3ox2*, and *KAO*. The GA signaling gene *OsGID1* served as a negative GA-responsive control. As shown in Figure 5B, transgenic plants overexpressed similar levels of OsINO80-YFP and YFP (P_{UBI}*::YFP*) (Jin et al. 2015). ChIP analyses showed that OsINO80-YFP especially enriches at the 5' and 3' transcribed regions of the *CPS1* and *GA3ox2* genes, compared with the negative control YFP (Figure 5C and 5D), but not at those of *KAO* or *OsGID1* (Figure S6C and S6D), indicating that *CPS1* and *GA3ox2* are the direct target genes of OsINO80, but *KAO* and *OsGID1* are not. The up-regulation of *KAO* in *OsINO80*-knockdown mutants appears similar to that in some GA deficient mutants, such as *gibberellin-deficient dwarf1* (*gdd1*) (Li et al. 2011), and the discrepancy between *KAO* expression and GA levels might be due to secondary effects and/or a post-transcriptional mechanism regulating the KAO protein

level or function. Taken together, we conclude that OsINO80 directly binds to the GA biosynthesis genes *CPS1* and *GA3ox2*, and maintains their expression level possibly through chromatin remodeling.

OsINO80 affects H2A.Z enrichment at GA biosynthesis genes

The next question is what will happen after OsINO80 enrichment at its target genes? H2A.Z is known as an H2A variant that performs essential functions in eukaryotes, and its dynamics are regulated and controlled by the ATP-dependent chromatin-remodeling complexes (Sarma and Reinberg 2005; Gerhold and Gasser 2014; Jarillo and Pineiro 2015). H2A.Z enriches at both active and silent genes, and may develop contrary transcription-related regulatory functions in a context-dependent manner (Jarillo and Pineiro 2015; Subramanian et al. 2015). The yeast INO80 acquires a histone-exchange activity by replacing nucleosomal H2A.Z/H2B with free H2A/H2B dimers (Papamichos-Chronakis et al. 2011). A recent study demonstrated that Arabidopsis INO80 interacts with H2A.Z and promotes key flowering genes' expression (Zhang et al. 2015). Therefore, we investigated the relationship between OsINO80 and H2A.Z in rice. We expressed a fragment of OsINO80 (299–567 AA) fused to a glutathione S-transferase (GST) tag. Using an *in vitro* pulldown assay, we found that GST-fused OsINO80, but not GST alone, preferentially interacted with H2A.Z (Figure 6A).

We find that the polyclonal antibodies against Arabidopsis H2A.Z (Zhang et al. 2015) did not efficiently recognize rice H2A.Z (OsH2A.Z), probably because that several amino acids in the peptides of Arabidopsis H2A.Z used as the antigen are different from those in the rice H2A.Z. So we produced the specific antibody against rice H2A.Z using the peptides within HTA705 and HTA713 to verify the *in planta* interaction between OsINO80 and rice H2A.Z. As shown in Figure S7A, the OsH2A.Z antibody distinctively recognized the two typical rice H2A.Z proteins (HTA705 and 713) but not the H2A proteins (HTA702, 704 and 707) in western blot analysis. By using the rice mesophyll protoplasts overexpressing either the FLAG-tagged OsH2A (HTA702) or HA-tagged OsH2A.Z (HTA705) fusion proteins, only OsH2A.Z but not OsH2A could be recognized by the rice H2A.Z antibody (Figure S7B), further demonstrating the specificity of the antibody against OsH2A.Z. Using this rice H2A.Z antibody and the commercial H2A antibody, we performed a co-immunoprecipitation (Co-IP) experiment. The

rice H2A.Z, but not H2A, was detected in the OsINO80-YFP immunoprecipitated fraction from the transgenic rice expressing *OsINO80-YFP* (Figure 6B), further confirming the physical interaction between OsINO80 and OsH2A.Z *in vivo*.

Using the rice H2A.Z antibody, ChIP-PCR analyses were performed in wild-type rice and *OsINO80*-knockdown mutants. We found that H2A.Z enriches near the 5' and 3' transcribed regions of *CPS1* and *GA3ox2* genes in the wild-type plants (Figure 6C and 6D). Upon the knockdown of *OsINO80*, H2A.Z enrichments at the chromatin of *GA3ox2* decreased obviously in both the T-DNA insertion mutant *osino80/+* and RNAi mutant *osino80Ri-2*, similarly a decrease of H2A.Z enrichment at *CPS1* was also observed (Figure 6C and 6D). In contrast, the levels of H2A.Z at *OsGID1* chromatin in the *OsINO80*-knockdown mutants were similar to those in the wild-type plants (Figure S8). When using the H3 antibody, H3 distribution patterns in *CPS1* and *GA3ox2* genes were observed similarly in wild-type and *OsINO80*-knockdown mutants (Figure 6C and 6D), indicating that OsINO80 does not affect the nucleosome positioning of its target genes. In *OsINO80*-knockdown mutants, the decreased H2A.Z but unchanged H3 distribution patterns at *CPS1* and *GA3ox2*, combined with the down-regulation of these two genes, indicate that OsINO80 affects gene transcription in the GA biosynthesis pathway by altering H2A.Z deposition but not nucleosome occupancy.

DISCUSSION

Several Arabidopsis chromatin-remodeling factors, such as BRM, SWI3C, and PKL, have been reported to function in the GA pathway (Henderson 2004; Archacki et al. 2013; Zhang et al. 2014). Here, we showed that both T-DNA insertion and RNAi mutants of *OsINO80* displayed typical GA-deficient phenotypes, and the addition of exogenous GA_3 rescued the young seedling's dwarf phenotype of the mutants. Consistently, in the *OsINO80*-knockdown mutants, the GA biosynthesis genes *CPS1* and *GA3ox2* were down-regulated. *CPS1* encodes an enzyme that catalyzes an early step in the GA biosynthetic pathway, producing GA_{12} (Sakamoto 2004). The levels of endogenous GA_{12} and the subsequent GAs, including GA_{53}, GA_{19}, GA_{20} and bioactive GA_1, were all decreased in the *osino80Ri-2* mutant plants compared with those in the wild-type ones. Moreover, we found that OsINO80 protein directly binds to *CPS1* and *GA3ox2* and affects the H2A.Z deposition at these genes. Thus, our study establishes that OsINO80 is

directly involved in GA biosynthesis, providing a first evidence in rice linking the phytohormone GA pathway with a chromatin-remodeling mechanism of regulation.

Chromatin-remodeling factors usually use ATP hydrolysis to facilitate histone octamer sliding, to remove or exchange histones, and to alter nucleosome positioning and structure, which leads to a modified chromatin structure during gene regulation (Flaus and Owen-Hughes 2004). ChIP analyses using the histone H3 antibody showed that the *OsINO80*-knockdown mutants displayed similar patterns of nucleosome occupancy at *CPS1* and *GA3ox2* as the wild-type ones. Thus, OsINO80 affects the nucleosome composition of *CPS1* and *GA3ox2*, without altering the nucleosome positioning. Several reports in *Drosophila* (Rhee and Pugh 2012; Weber et al. 2014) and in Arabidopsis (Sura et al. 2017) suggest that H2A.Z at the +1 nucleosome correlates with transcription activation. While a recent work proposes that H2A.Z in gene body associates with transcription repression in Arabidopsis (Sura et al. 2017). For the OsINO80 target genes *CPS1* and *GA3ox2*, H2A.Z enrichments decrease both close to the +1 nucleosome and within 3' gene body in the *OsINO80*-knockdown mutants, so the down-regulation of these two genes are probably due to the synergistic effects. In the future, to determine how OsINO80 protein is recruited to the target genes of *CPS1* and *GA3ox2* will help us to further understand the molecular mechanisms underlying OsINO80 regulation of the rice GA pathway.

Our previous work (Zhang et al. 2015) and this study showed that AtINO80 and OsINO80 proteins share similar domain organization and H2A.Z specific binding activity, and they both affect plant height, flowering time and male gametophyte, but both genetic and molecular analyses indicate that AtINO80 and OsINO80 play also some different roles during plant growth and development. For example, when comparing the expressolog genes using the RNA-seq data of *osino80Ri-2* and the microarray data of *atino80-5*, we found that only 41 out of 767 down-regulated and 57 out of 938 up-regulated expressolog genes in *atino80-5* overlap respectively with those in *osino80Ri-2*, suggesting the different effects of AtINO80 and OsINO80 on gene transcription (Figure S9). Moreover, in contrast with the viable and fertile phenotypes of the Arabidopsis mutant *atino80-5* (Zhang et al. 2015), the *OsINO80* loss-of-function mutant displayed more severe defects in reproductive development and viability in rice. We believe that future work in identifying the specific target genes of AtINO80 and

OsINO80 will help us to understand their different biological roles.

We propose that OsINO80 is probably involved in GA-mediated pollen germination and pollen tube elongation, because GA plays important roles in pollen viability and pollen tube growth in rice (Chhun et al. 2007). However, we cannot exclude the possibility that OsINO80 may directly modulate some genes involved in reproductive development. Likewise, we also cannot exclude the possibility that OsINO80 may directly regulate the genes responsible for flowering control. Because *OsINO80* is widely expressed in different rice tissues, it will be interesting to investigate whether *OsINO80* directly regulates more genes related to different biological processes at the chromatin level. RNA-seq analyses indicate that OsINO80 is required for the proper expression of many genes involved in diverse metabolic, biological, and cellular processes. Remarkably, many down- or up-regulated genes in *OsINO80*-knockdown plants enrich in functions related to stress responses and other phytohormones such as salicylic acid (SA), jasmonic acid (JA), abscisic acid (ABA) and growth hormone auxin. Thus, the transcriptome data not only highlighted the broad roles of OsINO80, but also provided direction for the further exploration of this chromatin-remodeling factor's functions.

MATERIALS AND METHODS

Plant material and growth conditions

The T-DNA insertion mutant line of *OsINO80* (line PFG_1C-03165.R, generated from japonica-type cultivar 'Hwayoung') was obtained from the database of T-DNA insertion mutant populations (Yi and An 2013), and RNAi mutants have an *O. sativa* 'Nipponbare' background in this study. For phenotype analyses, plants were cultured in the paddy fields of Shanghai (LD photoperiod) and Sanya (SD photoperiod). Seedlings were grown in artificial growth chambers under LD conditions (30°C during 14-h light/28°C during 10-h dark) or SD conditions (30°C during 10-h light/28°C during 14-h dark) for molecular experiments.

Gene expression analysis

Two-week-old rice shoots were harvested for total RNA extraction using TRIzol reagent according to the manufacturer's instructions (Invitrogen; http://www.invitrogen.com). Reverse transcription was performed using Improm-II reverse transcriptase (Promega;

http://www.promega.com) according to the standard protocol provided. Using gene-specific primers listed in Table S3, qPCR was performed. *OsUbiquitin5* was used as the reference gene for data normalization.

GUS staining assay

The *OsINO80* promoter fragment containing 2,000 bp nucleotides upstream of ATG was amplified by PCR using the primers listed in Table S3. The resulting DNA fragment replaced the cauliflower mosaic virus 35S promoter of pCAMBIA1301 to yield the construct $P_{OsINO80}$*::GUS*, which was transformed into rice plants. Histochemical GUS assays using the transgenic plants of $P_{OsINO80}$*::GUS* were performed as previously described (Jefferson et al. 1987).

Southern blot analysis

Genomic DNA was extracted and independently digested with two different enzymes, *Eco*RV and *Hin*dIII. The DNA fragments were separated on a 1.0% agarose gel and transferred onto a nylon membrane (GE Healthcare; http://www.gelifesciences.com). Then Southern blot analysis was performed with the DIG-High Prime DNA Labeling and Detection Starter Kit II (Roche; http://www.roche-applied-science.com) using the hygromycin resistance gene as the probe.

Pollen-related assays

Pollen grains from the anthers of wild-type plants and *OsINO80*-knockdown mutants were analyzed by pollen I_2-KI and 4',6-diamidino-2-phenylindole staining, and were germinated *in vitro* according to a previously described protocol (Han et al. 2006; Chhun et al. 2007).

Transgene constructs and plant transformation

DNA fragments containing nucleotides 2,038 to 2,239 and 4,849 to 5,234 of the *OsINO80* transcript were amplified as inverted repeats to construct a hairpin structure using the primers listed in Table S3. The hairpin structures were inserted into the vector pHB with a double cauliflower mosaic virus 35S promoter, obtaining P_{35S}*::OsINO80-RNAi-1* and P_{35S}*::OsINO80-RNAi-2* RNAi vectors for plant transformations. The full-length cDNA of *OsINO80* was

amplified by qRT-PCR using the primers listed in Table S3. The PCR product fused with the sequence encoding-enhanced YFP was then cloned into the vector pU1301 with the maize Ubiquitin promoter, obtaining P_{UBI}*::OsINO80-YFP* for plant transformations. The plant transformations were performed using the *Agrobacterium tumefaciens* (strain EHA105)-mediated method described previously (Sun and Zhou 2008).

Bioinformatics analysis of RNA-seq data

The total RNA was extracted using TRIzol reagent (Invitrogen) from 2-week-old seedlings. Library construction and sequencing were performed as described previously (Liu et al. 2016). Mapping information of RNA-seq data was shown in Table S4. The original paired-end reads were first trimmed using CUTADAPT v1.10 (Martin 2011). Then, TOPHAT2 v2.0.13 (Kim et al. 2013) was used to align the adapter-removed raw reads to the complete reference genome of 'Nipponbare' (japonica) rice (http://rice.plantbiology.msu.edu). The normalized gene expression levels were calculated as fragments per kilobase of exon per million fragments mapped by CUFFLINKS v2.2.1 (Trapnell et al. 2010). Next, the differentially expressed genes (DEGs) were identified using the CUFFDIFF program, which is a subpackage of CUFFLINKS. The identification of the DEGs was performed at a threshold of more than twofold change and a P-value < 0.05.

For transcriptome comparison, the significant mis-regulated genes in Arabidopsis (Noh and Amasino 2003; Fritsch et al. 2004; Choi et al. 2007; Rosa et al. 2013; Zhang et al. 2015) were transformed to their homologous genes in rice firstly. Homologous genes data were downloaded from the web site (http://rice.plantbiology.msu.edu) and venn diagrams were generated with the 'Venn Diagram' packages in R software.

GO analysis

For the GO enrichment analysis, we uploaded the DEGs list to the online tool CARMO, which is a comprehensive annotation platform for the functional exploration of rice multi-omics data (http://bioinfo.sibs.ac.cn/carmo/Gene_Annotation.php) (Wang et al. 2015). The significantly enriched biological processes among the DEGs (P < 0.05) were identified in *OsINO80*-knockdown mutants.

Quantification of endogenous GAs

2-week-old seedlings (1 g) were frozen in liquid nitrogen, ground into fine powders and then 15 mL 80% (v/v) methanol extractions at 4°C for 12 h were performed. The endogenous GAs were analysed by the Greentek Corporation (http://www.greenswordcreation.com).

Exogenous GA_3 response assay

The seeds of wild-type rice and *OsINO80*-knockdown mutants were sterilized with 0.1% $HgCl_2$ for 15 min, washed four times using sterile distilled water, and finally planted on agar-solidified Murashige and Skoog medium containing 0, 10^{-10}, 10^{-8}, 10^{-6}, and 10^{-4} M bioactive GA_3. After 1 week, the lengths of second leaf sheaths were measured.

ChIP assays

2-week-old rice shoots were used in ChIP assays as previously described (Sui et al. 2012). Anti-histone H3 (ab1791) and anti-GFP (A-11122) were purchased from Abcam (http://www.abcam.com) and Invitrogen (http://www.invitrogen.com), respectively. The rabbit polyclonal antibodies specially recognized rice H2A.Z (OsH2A.Z) were generated against the mixed OsH2A.Z-specific peptides N-AGKGGKGLLAAKTTAAKAAADKDKDRKKAPVS-C (HTA705) and N-AGKGGKGLLAAKTTAAKSAEKDKGKKAPVS-C (HTA713) using a commercial service by Abmart (http://www.ab-mart.com.cn). Rice H2A (HTA702, 704, and 707) and H2A.Z (HTA705 and 713) cDNAs were amplified with primers listed in Table S3 and then cloned into the pGEX-4T-1 vector (Novagen; http://www.novagen.com). The purified rice H2A/H2A.Z proteins were used for detecting the recognition capacity of the OsH2A.Z antibody. The enrichments of immunoprecipitated DNAs were determined by qPCR using a kit from Takara (http://www.takara-bio.com). Gene-specific primers are listed in Table S3. The ChIP efficiency values are the ratios determined by taking a fixed aliquot of the DNA extracted from the immunoprecipitated samples and the ChIP input, and the fold change values in the figures are the normalized ChIP efficiency values using the reference gene *OsUbiquitin5* as the internal standard. Error bars show standard deviation from three paralleled biological replicates.

Protein binding assays

CDSs of histones H2A, H2B and H2A.Z were cloned into vector pET24a (Novagen; http://www.merckmillipore.com/). OsINO80 (299–567) cDNA was amplified using $OsINO80_{299–567}$-F/R (Table S3) and cloned into the pGEX-4T-1 vector to construct GST-fused OsINO80 proteins. Pulldown experiments were performed according to a previously described protocol (Bu et al. 2014). The antibodies against GST (M20007) were purchased from Abmart (http://www.ab-mart.com.cn).

Protoplast isolation, transformation and immunoprecipitation (IP) assays

Protoplast isolation and transformation were performed using one to two weeks old rice shoots as described previously (Choi et al. 2014). Rice H2A (HTA702) cDNA amplified using primers HTA702-PF/R was fused with FLAG cDNA and cloned into the pCAMBIA1300 vector driven by the cauliflower mosaic virus 35S promoter (*P_{35S}::FLAG-OsH2A*). Rice H2A.Z (HTA705) cDNA amplified using primers HTA705-PF/R was fused with HA cDNA and cloned into the pU1301 vector with the maize Ubiquitin promoter (*P_{UBI}::HA-OsH2A.Z*). The constructs were transformed into protoplasts and the extracts were immunoprecipitated by anti-FLAG (F1084; Sigma; http://www.sigmaaldrich.com) or anti-HA (ab9110; Abcam; http://www.abcam.com) antibodies. The immunoprecipitated fraction was further detected by western blotting using anti-FLAG, anti-HA or anti-OsH2A.Z antibodies.

Co-immunoprecipitation (Co-IP) assays

2-week-old rice shoots over-expressing *OsINO80-YFP* (*P_{UBI}::OsINO80-YFP*) in wild-type 'Nipponbare' background were used to perform a Co-IP assay as described previously (Molitor et al. 2014). The proteins were extracted in lysis buffer (50 mM Tris-HCl pH 8.0, 150 mM NaCl, 10% glycerol, 5 mM $MgCl_2$, 0.1% NP-40, 1 mM EDTA, 2 mM DTT, anti-complete proteinase (Roche; http://www.roche-applied-science.com)). IP was performed using anti-GFP (M20004; Abmart; http://www.ab-mart.com.cn) in combination with pre-cleared magnetic protein A beads (Magna-ChIP; Millipore; http://www.merckmillipore.com) at 4°C for 3 h. After washing, the input and immunoprecipitated fractions were detected by western blotting using anti-GFP, anti-H2A (ab18255; Abcam; http://www.abcam.com) or anti-

OsH2A.Z antibodies.

Data access

The RNA-seq data have been deposited in the NCBI SRA database (http://www.ncbi.nlm.nih.gov/sra) with the accession number SRP????.

ACKNOWLEDGEMENTS

This work was supported by the National Basic Research Program of China (973 Program, Grants no. 2012CB910500) and the National Natural Science Foundation of China (31570315, 91519308, and 31371304).

AUTHOR CONTRIBUTIONS

A.D. conceived the project; C.L. performed most of the experiments; Y.L. performed the library construction and bioinformatics analyses of RNA-seq data; C.L., Y.L., Y.Y. and A.D. analyzed the data; C.L., WH.S., Y.Y. and A.D. wrote the paper.

REFERENCES

Archacki R, Buszewicz D, Sarnowski TJ, Sarnowska E, Rolicka AT, Tohge T, Fernie AR, Jikumaru Y, Kotlinski M, Iwanicka-Nowicka R, Kalisiak K, Patryn J, Halibart-Puzio J, Kamiya Y, Davis SJ, Koblowska MK, Jerzmanowski A (2013) BRAHMA ATPase of the SWI/SNF Chromatin Remodeling Complex Acts as a Positive Regulator of Gibberellin-Mediated Responses in Arabidopsis. **PLoS ONE** 8: e58588

Bu Z, Yu Y, Li Z, Liu Y, Jiang W, Huang Y, Dong AW (2014) Regulation of arabidopsis flowering by the histone mark readers MRG1/2 via interaction with CONSTANS to modulate FT expression. **PLoS Genet** 10: e1004617

Chhun T, Aya K, Asano K, Yamamoto E, Morinaka Y, Watanabe M, Kitano H, Ashikari M, Matsuoka M, Ueguchi-Tanaka M (2007) Gibberellin regulates pollen viability and pollen tube growth in rice. **Plant Cell** 19: 3876-3888

Choi K, Park C, Lee J, Oh M, Noh B, Lee I (2007) Arabidopsis homologs of components of the SWR1 complex regulate flowering and plant development. **Development** 134: 1931-1941

Choi SC, Lee S, Kim SR, Lee YS, Liu C, Cao X, An G (2014) Trithorax group protein Oryza sativa Trithorax1 controls flowering time in rice via interaction with early heading date3. **Plant Physiol** 164: 1326-1337

Clapier CR, Cairns BR (2009) The biology of chromatin remodeling complexes. **Annu Rev Biochem** 78: 273-304

Flaus A, Owen-Hughes T (2004) Mechanisms for ATP-dependent chromatin remodelling: farewell to the tuna-can octamer? **Curr Opin Genet Dev** 14: 165-173

Fritsch O, Benvenuto G, Bowler C, Molinier J, Hohn B (2004) The INO80 protein controls homologous recombination in Arabidopsis thaliana. **Mol Cell** 16: 479-485

Gerhold CB, Gasser SM (2014) INO80 and SWR complexes: relating structure to function in chromatin remodeling. **Trends Cell Biol** 24: 619-631

Han MJ, Jung KH, Yi G, Lee DY, An G (2006) Rice Immature Pollen 1 (RIP1) is a regulator of late pollen development. **Plant Cell Physiol** 47: 1457-1472

Hedden P, Sponsel V (2015) A Century of Gibberellin Research. **J Plant Growth Regul** 34: 740-760

Henderson JT (2004) PICKLE Acts throughout the Plant to Repress Expression of Embryonic Traits and May Play a Role in Gibberellin-Dependent Responses. **Plant Physiol** 134: 995-1005

Hu Y, Liu D, Zhong X, Zhang C, Zhang Q, Zhou DX (2012) CHD3 protein recognizes and regulates methylated histone H3 lysines 4 and 27 over a subset of targets in the rice genome. **Proc Natl Acad Sci U S A** 109: 5773-5778

Huanca-Mamani W, Garcia-Aguilar M, Leon-Martinez G, Grossniklaus U, Vielle-Calzada JP (2005) CHR11, a chromatin-remodeling factor essential for nuclear proliferation during female gametogenesis in Arabidopsis thaliana. **Proc Natl Acad Sci U S A** 102: 17231-17236

Jarillo JA, Pineiro M (2015) H2A.Z mediates different aspects of chromatin function and modulates flowering responses in Arabidopsis. **Plant J** 83: 96-109

Jefferson RA, Kavanagh TA, Bevan MW (1987) GUS fusions: beta-glucuronidase as a sensitive and versatile gene fusion marker in higher plants. **EMBO J** 6: 3901-3907

Jin J, Shi J, Liu B, Liu Y, Huang Y, Yu Y, Dong A (2015) MORF-RELATED GENE702, a Reader Protein of Trimethylated Histone H3 Lysine 4 and Histone H3 Lysine 36, Is Involved in Brassinosteroid-Regulated Growth and Flowering Time Control in Rice. **Plant Physiol** 168: 1275-1285

Kim D, Pertea G, Trapnell C, Pimentel H, Kelley R, Salzberg SL (2013) TopHat2: accurate alignment of transcriptomes in the presence of insertions, deletions and gene fusions. **Genome Biol** 14: R36

Li G, Liu S, Wang J, He J, Huang H, Zhang Y, Xu L (2014) ISWI proteins participate in the genome-wide nucleosome distribution in Arabidopsis. **Plant J** 78: 706-714

Li G, Zhang J, Li J, Yang Z, Huang H, Xu L (2012) Imitation Switch chromatin remodeling factors and their interacting RINGLET proteins act together in controlling the plant vegetative phase in Arabidopsis. **Plant J** 72: 261-270

Li H, Durbin R (2009) Fast and accurate short read alignment with Burrows-Wheeler transform. **Bioinformatics** 25: 1754-1760

Li H, Handsaker B, Wysoker A, Fennell T, Ruan J, Homer N, Marth G, Abecasis G, Durbin R (2009) The Sequence Alignment/Map format and SAMtools. **Bioinformatics** 25: 2078-2079

Li J, Jiang J, Qian Q, Xu Y, Zhang C, Xiao J, Du C, Luo W, Zou G, Chen M, Huang Y, Feng Y, Cheng Z, Yuan M, Chong K (2011) Mutation of rice BC12/GDD1, which encodes a kinesin-like protein that binds to a GA biosynthesis gene promoter, leads to dwarfism with impaired cell elongation. **Plant Cell** 23: 628-640

Liu B, Wei G, Shi J, Jin J, Shen T, Ni T, Shen W-H, Yu Y, Dong A (2016) SET DOMAIN GROUP 708, a histone H3 lysine 36-specific methyltransferase, controls flowering time in rice (Oryza sativa). **New Phytol** 210: 577-588

Martin M (2011) Cutadapt removes adapter sequences from high-throughput sequencing reads. **Embnet J** 17: 10-12

Molitor AM, Bu Z, Yu Y, Shen WH (2014) Arabidopsis AL PHD-PRC1 complexes promote seed germination through H3K4me3-to-H3K27me3 chromatin state switch in repression of seed

developmental genes. **PLoS Genet** 10: e1004091

Noh YS, Amasino RM (2003) PIE1, an ISWI family gene, is required for FLC activation and floral repression in Arabidopsis. **Plant Cell** 15: 1671-1682

Papamichos-Chronakis M, Watanabe S, Rando OJ, Peterson CL (2011) Global regulation of H2A.Z localization by the INO80 chromatin-remodeling enzyme is essential for genome integrity. **Cell** 144: 200-213

Quinlan AR, Hall IM (2010) BEDTools: a flexible suite of utilities for comparing genomic features. **Bioinformatics** 26: 841-842

Ramirez F, Ryan DP, Gruning B, Bhardwaj V, Kilpert F, Richter AS, Heyne S, Dundar F, Manke T (2016) deepTools2: a next generation web server for deep-sequencing data analysis. **Nucleic Acids Res** 44: W160-165

Rhee HS, Pugh BF (2012) Genome-wide structure and organization of eukaryotic pre-initiation complexes. **Nature** 483: 295-301

Robinson JT, Thorvaldsdottir H, Winckler W, Guttman M, Lander ES, Getz G, Mesirov JP (2011) Integrative genomics viewer. **Nat Biotechnol** 29: 24-26

Rosa M, Von Harder M, Cigliano RA, Schlogelhofer P, Mittelsten Scheid O (2013) The Arabidopsis SWR1 chromatin-remodeling complex is important for DNA repair, somatic recombination, and meiosis. **Plant Cell** 25: 1990-2001

Sakamoto T (2004) An Overview of Gibberellin Metabolism Enzyme Genes and Their Related Mutants in Rice. **Plant Physiol** 134: 1642-1653

Sarma K, Reinberg D (2005) Histone variants meet their match. **Nat Rev Mol Cell Biol** 6: 139-149

Sarnowska EA, Rolicka AT, Bucior E, Cwiek P, Tohge T, Fernie AR, Jikumaru Y, Kamiya Y, Franzen R, Schmelzer E, Porri A, Sacharowski S, Gratkowska DM, Zugaj DL, Taff A, Zalewska A, Archacki R, Davis SJ, Coupland G, Koncz C, Jerzmanowski A, Sarnowski TJ (2013) DELLA-Interacting SWI3C Core Subunit of Switch/Sucrose Nonfermenting Chromatin Remodeling Complex Modulates Gibberellin Responses and Hormonal Cross Talk in Arabidopsis. **Plant Physiol** 163: 305-317

Subramanian V, Fields PA, Boyer LA (2015) H2A.Z: a molecular rheostat for transcriptional control. **F1000Prime Reports** 7

Sui P, Jin J, Ye S, Mu C, Gao J, Feng H, Shen W-H, Yu Y, Dong A (2012) H3K36 methylation is critical for brassinosteroid-regulated plant growth and development in rice. **Plant J** 70: 340-347

Sun Q, Zhou DX (2008) Rice jmjC domain-containing gene JMJ706 encodes H3K9 demethylase required for floral organ development. **Proc Natl Acad Sci U S A** 105: 13679-13684

Sun T-p (2008) Gibberellin Metabolism, Perception and Signaling Pathways in Arabidopsis. The **Arabidopsis Book** 6: e0103

Sura W, Kabza M, Karlowski WM, Bieluszewski T, Kus-Slowinska M, Paweloszek L, Sadowski J, Ziolkowski PA (2017) Dual Role of the Histone Variant H2A.Z in Transcriptional Regulation of Stress-Response Genes. **Plant Cell** 29: 791-807

Trapnell C, Williams BA, Pertea G, Mortazavi A, Kwan G, van Baren MJ, Salzberg SL, Wold BJ, Pachter L (2010) Transcript assembly and quantification by RNA-Seq reveals unannotated transcripts and isoform switching during cell differentiation. **Nat Biotechnol** 28: 511-515

Ueguchi-Tanaka M, Nakajima M, Motoyuki A, Matsuoka M (2007) Gibberellin Receptor and Its Role in Gibberellin Signaling in Plants. **Annu Rev Plant Biol** 58: 183-198

Wang J, Qi M, Liu J, Zhang Y (2015) CARMO: a comprehensive annotation platform for functional exploration of rice multi-omics data. **Plant J** 83: 359-374

Weber CM, Ramachandran S, Henikoff S (2014) Nucleosomes are context-specific, H2A.Z-modulated barriers to RNA polymerase. **Mol Cell** 53: 819-830

Yamaguchi S (2008) Gibberellin Metabolism and its Regulation. **Annu Rev Plant Biol** 59: 225-251

Yelagandula R, Stroud H, Holec S, Zhou K, Feng S, Zhong X, Muthurajan Uma M, Nie X, Kawashima T, Groth M, Luger K, Jacobsen Steven E, Berger F (2014) The Histone Variant H2A.W Defines Heterochromatin and Promotes Chromatin Condensation in Arabidopsis. **Cell** 158: 98-109

Yi J, An G (2013) Utilization of T-DNA tagging lines in rice. **J Plant Biol** 56: 85-90

Zhang C, Cao L, Rong L, An Z, Zhou W, Ma J, Shen W-H, Zhu Y, Dong A (2015) The chromatin-remodeling factor AtINO80 plays crucial roles in genome stability maintenance and in plant development. **Plant J** 82: 655-668

Zhang D, Jing Y, Jiang Z, Lin R (2014) The Chromatin-Remodeling Factor PICKLE Integrates Brassinosteroid and Gibberellin Signaling during Skotomorphogenic Growth in Arabidopsis. **Plant Cell** 26: 2472-2485

Zhang K, Xu W, Wang C, Yi X, Zhang W, Su Z (2017) Differential deposition of H2A.Z in combination with histone modifications within related genes in Oryza sativa callus and seedling. **Plant J** 89: 264-277

Zhao C, Xu J, Chen Y, Mao C, Zhang S, Bai Y, Jiang D, Wu P (2012) Molecular cloning and characterization of OsCHR4, a rice chromatin-remodeling factor required for early chloroplast development in adaxial mesophyll. **Planta** 236: 1165-1176

Table 1. Reciprocal crosses between *osino80/+* and wild-type ‘Hwayoung’.

Crosses (male × female)	Total Number in F1	Number of *osino80/+* in F1	Number of Hwayoung in F1	Observed Ratio	Expected Ratio	χ^2-test Result
osino80/+ ×Hwayoung	114	17	97	0.175:1	1:1	χ^2-value=28.070 (*p*-value<0.01)
Hwayoung × *osino80/+*	73	32	41	0.780:1	1:1	χ^2-value=1.110 (*p*-value>0.05)
Hwayoung × Hwayoung	94	0	94			

FIGURE LEGENDS

Figure 1. Characterization of T-DNA insertion mutant of *Oryza sativa INO80*.

(A) Schematic representation of the *OsINO80* gene structure and the T-DNA insertion in the line PFG_1C-03165.R. Black and gray boxes indicate for the coding sequences and untranslated regions, respectively. The right T-DNA border primer (RB) is located at the 3' end of the insertion. LP and RP are the left and right genomic primers, respectively, which were designed based on the *OsINO80* sequence.

(B) Southern blot analysis. Genomic DNA of the wild-type 'Hwayoung' and the mutant *osino80/+* were digested using the restriction enzyme *Eco*RV or *Hin*dIII, and were analyzed through hybridizing using a hygromycin resistance gene as probe.

(C) PCR amplification from genomic DNA of wild-type 'Hwayoung' and heterozygous *osino80/+* plants using LP/RP and RB/RP primer pairs, respectively.

(D) The segregation ratio of the progeny from self-pollinated heterozygous *osino80/+* plants.

(E) Relative expression levels of *OsINO80*. *OsUbiquitin5* served as the internal control. Values shown are means ± standard deviations (SDs) of three independent replicates. Asterisks indicate statistically significant differences between *osino80/+* and the wild-type 'Hwayoung' ($P < 0.05$).

(F) Overall morphologies of the wild-type 'Hwayoung' and the mutant *osino80/+*. Bar = 15 cm.

(G) Lengths of panicles and internodes of wild-type 'Hwayoung' and mutant *osino80/+* plants.

(H) Cell lengths in the second leaf sheaths of wild-type 'Hwayoung' and mutant *osino80/+* plants. Asterisks indicate statistically significant differences between *osino80/+* and the wild-type 'Hwayoung' ($P < 0.05$).

(I) Heading time of the wild-type 'Hwayoung' and the mutant *osino80/+* plants grown under LD (Shanghai) conditions. Values shown are means ± SDs (n = 30). Asterisks indicate statistically significant differences between *osino80/+* and the wild-type 'Hwayoung' ($P < 0.05$).

Figure 2. OsINO80 is required for pollen germination and pollen tube elongation.

(A) Pollen grains stained dark by I_2-KI solution. Bar = 100 μm.

(B) Pollen grains stained by 4',6-diamidino-2-phenylindole. V, vegetative nuclei; S, sperm

nuclei; Gp, germination pore. Bar = 50 μm.

(C) Pollen germination assays with pollen grains collected from the wild-type ‘Hwayoung’ and the *osino80/+* plants. Bar = 50 μm.

(D) Pollen germination rates in the wild-type ‘Hwayoung’ and the *osino80/+* mutant.

Figure 3. RNA interference of *OsINO80* impairs rice growth and disturbs gene expression in multiple processes.

(A) Overall morphologies of the wild-type ‘Nipponbare’ and the mutant *osino80Ri-1* and *osino80Ri-2* plants. Bar = 15 cm.

(B) Relative expression levels of *OsINO80*. *OsUbiquitin5* served as the internal control. Values shown are means ± SDs of three independent replicates. Asterisks indicate statistically significant differences between the RNAi plants and the wild-type ‘Nipponbare’ ($P < 0.05$).

(C) Significant enriched biological processes identified by a gene ontology (GO) analysis of the down-regulated genes in the mutant *osino80Ri-2* ($P < 0.05$).

(D) Significant enriched biological processes identified by a GO analysis of the up-regulated genes in *osino80Ri-2* ($P < 0.05$).

(E–H) RNA-seq data showing the transcription levels of *OsINO80* (E), *CPS1* (F), *GA3ox2* (G), and *OsGID1* (H) in the wild-type ‘Nipponbare’ and *osino80Ri-2.*

Figure 4. OsINO80 is involved in regulation of the gibberellin (GA) biosynthesis pathway.

(A) Relative expression levels of GA-related genes in the wild-type ‘Nipponbare’ and the mutant *osino80Ri-2*. *OsUbiquitin5* served as the internal control, and the fold change relative to the wild-type level is shown. Values shown are means ± SDs from three independent replicates. Asterisks indicate statistically significant differences between *osino80Ri-2* and the wild-type plants ($P < 0.05$).

(B) The endogenous levels of GAs in the wild-type ‘Nipponbare’ and the mutant *osino80Ri-2* plants. The numbers boxed are endogenous GAs levels in wild-type ‘Nipponbare’ (black) and *osino80Ri-2* plants (orange). Data represent the means ±SD from three independent replicates in each line. Unit: ng•g-1 fresh weight; n.d., not detected; n.q., not quantified.

(C) Effects of different concentrations of GA_3 on the wild-type ‘Nipponbare’ and the mutant

osino80Ri-2. The lengths of the second leaf sheaths were measured. Values are means ± SDs (n = 20). Asterisks indicate statistically significant differences between *osino80Ri-2* and the wild-type 'Nipponbare' ($P < 0.05$).

Figure 5. OsINO80-YFP directly targets the GA biosynthesis genes *CPS1* and *GA3ox2*.

(A) Subcellular localization of OsINO80-YFP in rice root cells. Bar = 10 μm.

(B) Protein levels of YFP or OsINO80-YFP in the indicated genotypes detected by the GFP antibody.

(C) Enrichment of OsINO80-YFP at *CPS1* chromatin as analyzed by ChIP using GFP antibodies. Diagram representing *CPS1* gene structure. Bars labeled 1–11 represent regions amplified by PCR. Error bars show the SDs from three biological replicates.

(D) Enrichment of OsINO80-YFP at *GA3ox2* chromatin as analyzed by ChIP using GFP antibodies. Diagram representing *GA3ox2* gene structure. Bars labeled 1–7 represent regions amplified by PCR. Error bars show the SDs from three biological replicates.

Figure 6. OsINO80 interacts with OsH2A.Z and affects OsH2A.Z enrichment at the GA biosynthesis genes *CPS1* and *GA3ox2*.

(A) Pulldown assays demonstrating the interaction of purified GST-tagged OsINO80 with H2A/H2B or H2A.Z/H2B recombinant proteins expressed in *Escherichia coli*.

(B) Co-immunoprecipitation (Co-IP) detection of OsINO80 and OsH2A.Z interaction *in planta*. Total protein extracts from rice plants expressing *OsINO80-YFP* were immunoprecipitated with anti-GFP affinity beads and the resulting fractions were then analyzed by western blot using the antibodies against H2A or OsH2A.Z.

(C) ChIP analysis using antibodies against OsH2A.Z or H3 at *CPS1* chromatin in the indicated genotypes. Error bars show the SDs from three biological replicates.

(D) ChIP analysis using antibodies against OsH2A.Z or H3 at *GA3ox2* chromatin in the indicated genotypes. Error bars show the SDs from three biological replicates.

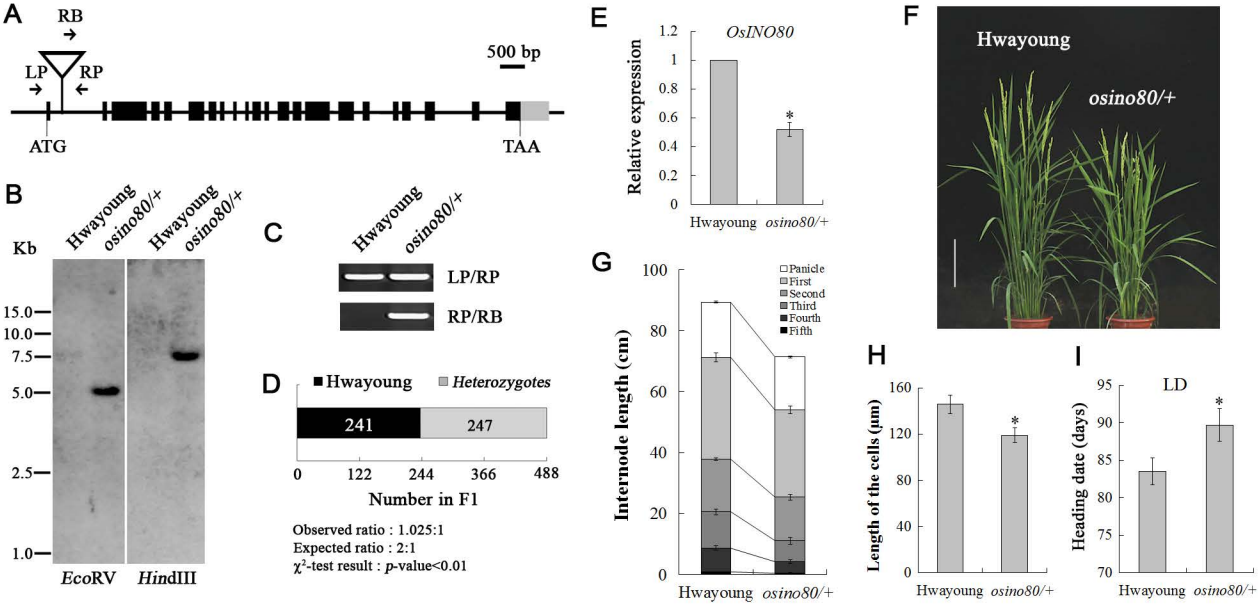

Figure 1. Characterization of T-DNA insertion mutant of *Oryza sativa INO80*.

(A) Schematic representation of the *OsINO80* gene structure and the T-DNA insertion in the line PFG_1C-03165.R. Black and gray boxes indicate for the coding sequences and untranslated regions, respectively. The right T-DNA border primer (RB) is located at the 3' end of the insertion. LP and RP are the left and right genomic primers, respectively, which were designed based on the *OsINO80* sequence.

(B) Southern blot analysis. Genomic DNA of the wild-type 'Hwayoung' and the mutant *osino80/+* were digested using the restriction enzyme *Eco*RV or *Hin*dIII, and were analyzed through hybridizing using a hygromycin resistance gene as probe.

(C) PCR amplification from genomic DNA of wild-type 'Hwayoung' and heterozygous *osino80/+* plants using LP/RP and RB/RP primer pairs, respectively.

(D) The segregation ratio of the progeny from self-pollinated heterozygous *osino80/+* plants.

(E) Relative expression levels of *OsINO80*. *OsUbiquitin5* served as the internal control. Values shown are means ± standard deviations (SDs) of three independent replicates. Asterisks indicate statistically significant differences between *osino80/+* and the wild-type 'Hwayoung' ($P < 0.05$).

(F) Overall morphologies of the wild-type 'Hwayoung' and the mutant *osino80/+*. Bar = 15 cm.

(G) Lengths of panicles and internodes of wild-type 'Hwayoung' and mutant *osino80/+* plants.

(H) Cell lengths in the second leaf sheaths of wild-type 'Hwayoung' and mutant *osino80/+* plants. Asterisks indicate statistically significant differences between *osino80/+* and the wild-type 'Hwayoung' ($P < 0.05$).

(I) Heading time of the wild-type 'Hwayoung' and the mutant *osino80/+* plants grown under LD (Shanghai) conditions. Values shown are means ± SDs (n = 30). Asterisks indicate statistically significant differences between *osino80/+* and the wild-type 'Hwayoung' ($P < 0.05$).

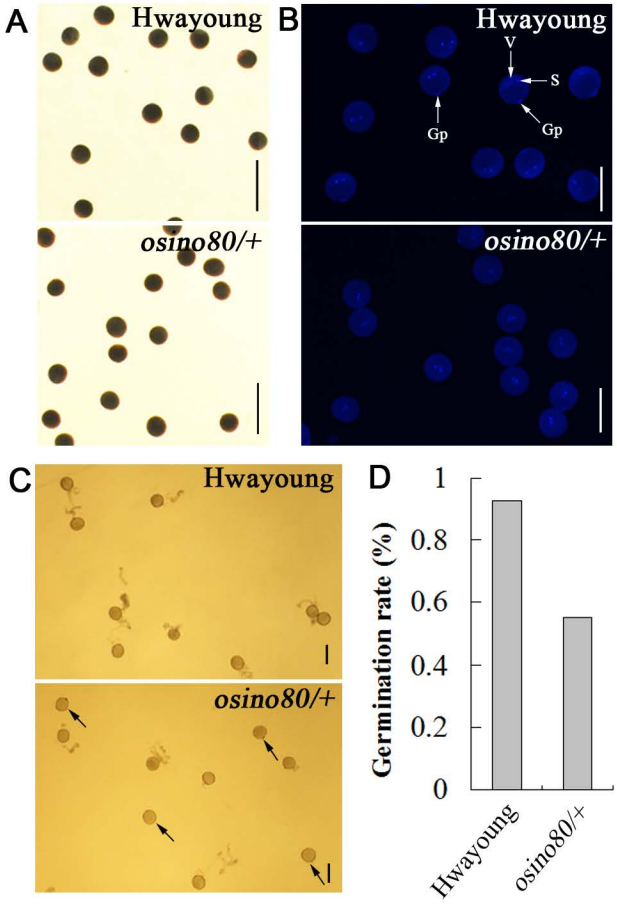

Figure 2. OsINO80 is required for pollen germination and pollen tube elongation.

(A) Pollen grains stained dark by I2-KI solution. Bar = 100 μm.

(B) Pollen grains stained by 4',6-diamidino-2-phenylindole. V, vegetative nuclei; S, sperm nuclei; Gp, germination pore. Bar = 50 μm.

(C) Pollen germination assays with pollen grains collected from the wild-type 'Hwayoung' and the *osino80/+* plants. Bar = 50 μm.

(D) Pollen germination rates in the wild-type 'Hwayoung' and the *osino80/+* mutant.

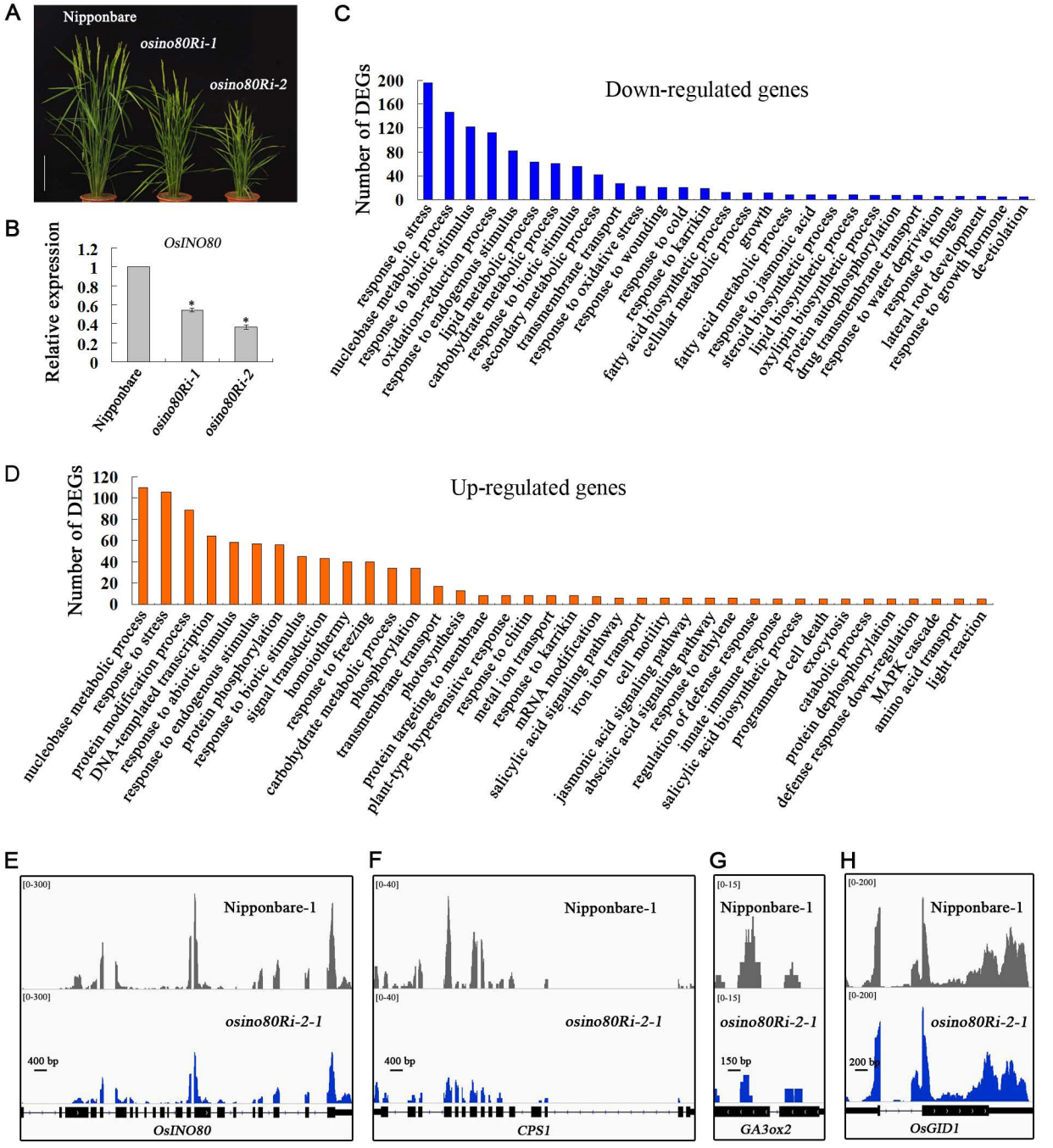

Figure 3. RNA interference of OsINO80 impairs rice growth and disturbs gene expression in multiple processes.

(A) Overall morphologies of the wild-type 'Nipponbare' and the mutant *osino80Ri-1* and *osino80Ri-2* plants. Bar = 15 cm.

(B) Relative expression levels of *OsINO80*. *OsUbiquitin5* served as the internal control. Values shown are means ± SDs of three independent replicates. Asterisks indicate statistically significant differences between the RNAi plants and the wild-type 'Nipponbare' ($P < 0.05$).

(C) Significant enriched biological processes identified by a gene ontology (GO) analysis of the down-regulated genes in the mutant *osino80Ri-2* ($P < 0.05$).

(D) Significant enriched biological processes identified by a GO analysis of the up-regulated genes in *osino80Ri-2* ($P < 0.05$).

(E–H) RNA-seq data showing the transcription levels of *OsINO80* (E), *CPS1* (F), *GA3ox2* (G), and *OsGID1* (H) in the wild-type 'Nipponbare' and *osino80Ri-2*.

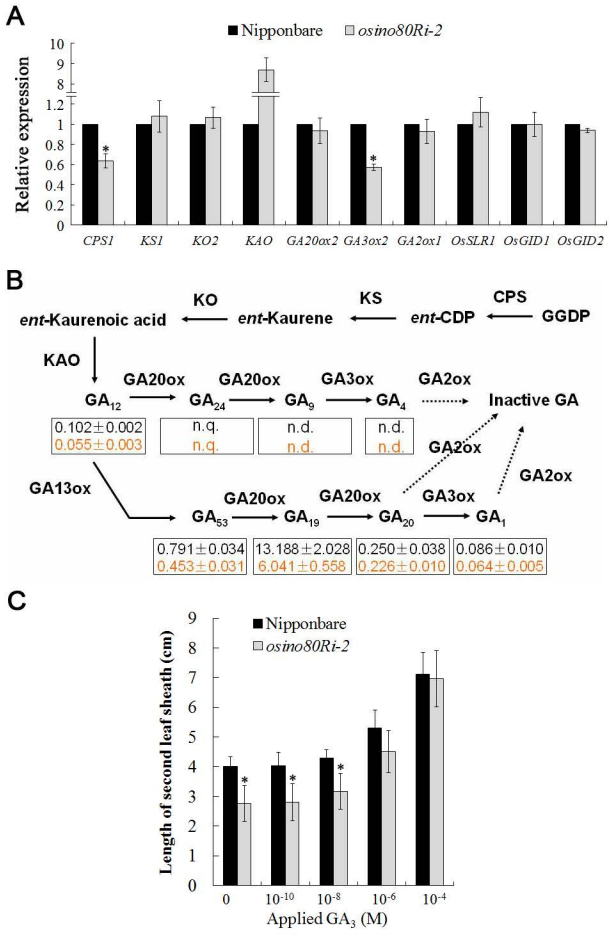

Figure 4. OsINO80 is involved in regulation of the gibberellin (GA) biosynthesis pathway.

(A) Relative expression levels of GA-related genes in the wild-type 'Nipponbare' and the mutant *osino80Ri-2*. *OsUbiquitin5* served as the internal control, and the fold change relative to the wild-type level is shown. Values shown are means ± SDs from three independent replicates. Asterisks indicate statistically significant differences between *osino80Ri-2* and the wild-type plants ($P < 0.05$).

(B) The endogenous levels of GAs in the wild-type 'Nipponbare' and the mutant *osino80Ri-2* plants. The numbers boxed are endogenous GAs levels in wild-type 'Nipponbare' (black) and *osino80Ri-2* plants (orange). Data represent the means ±SD from three independent replicates in each line. Unit: ng•g-1 fresh weight; n.d., not detected; n.q., not quantified.

(C) Effects of different concentrations of GA3 on the wild-type 'Nipponbare' and the mutant *osino80Ri-2*. The lengths of the second leaf sheaths were measured. Values are means ± SDs (n = 20). Asterisks indicate statistically significant differences between *osino80Ri-2* and the wild-type 'Nipponbare' ($P < 0.05$).

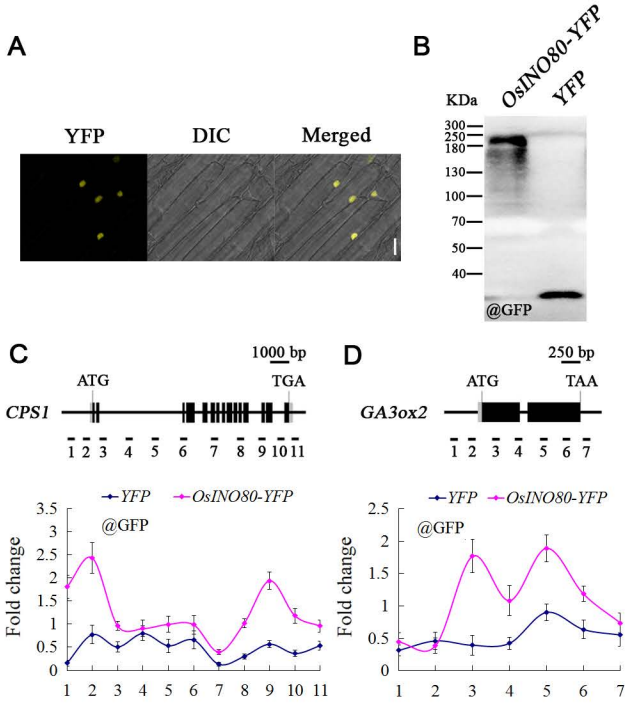

Figure 5. OsINO80-YFP directly targets the GA biosynthesis genes *CPS1* and *GA3ox2*.

(A) Subcellular localization of OsINO80-YFP in rice root cells. Bar = 10 μm.

(B) Protein levels of YFP or OsINO80-YFP in the indicated genotypes detected by the GFP antibody.

(C) Enrichment of OsINO80-YFP at *CPS1* chromatin as analyzed by ChIP using GFP antibodies. Diagram representing *CPS1* gene structure. Bars labeled 1–11 represent regions amplified by PCR. Error bars show the SDs from three biological replicates.

(D) Enrichment of OsINO80-YFP at *GA3ox2* chromatin as analyzed by ChIP using GFP antibodies. Diagram representing *GA3ox2* gene structure. Bars labeled 1–7 represent regions amplified by PCR. Error bars show the SDs from three biological replicates.

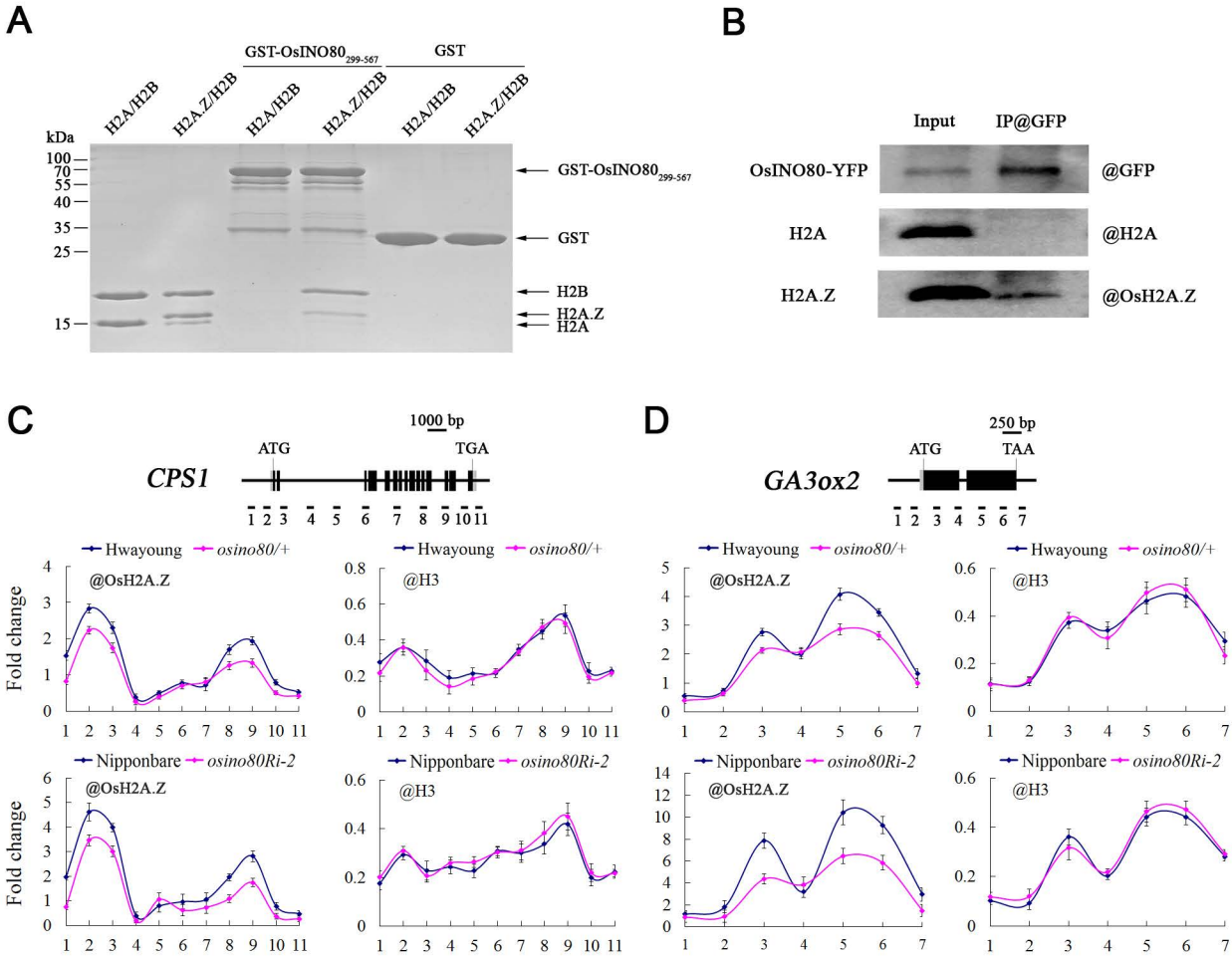

Figure 6. OsINO80 interacts with OsH2A.Z and affects OsH2A.Z enrichment at the GA biosynthesis genes *CPS1* and *GA3ox2*.

(A) Pulldown assays demonstrating the interaction of purified GST-tagged OsINO80 with H2A/H2B or H2A.Z/H2B recombinant proteins expressed in *Escherichia coli*.

(B) Co-immunoprecipitation (Co-IP) detection of OsINO80 and OsH2A.Z interaction *in planta*. Total protein extracts from rice plants expressing *OsINO80-YFP* were immunoprecipitated with anti-GFP affinity beads and the resulting fractions were then analyzed by western blot using the antibodies against H2A or OsH2A.Z.

(C) ChIP analysis using antibodies against OsH2A.Z or H3 at *CPS1* chromatin in the indicated genotypes. Error bars show the SDs from three biological replicates.

(D) ChIP analysis using antibodies against OsH2A.Z or H3 at *GA3ox2* chromatin in the indicated genotypes. Error bars show the SDs from three biological replicates.

SUPPORTING INFORMATION

Additional Supporting Information may be found online in the supporting information tab for this article:

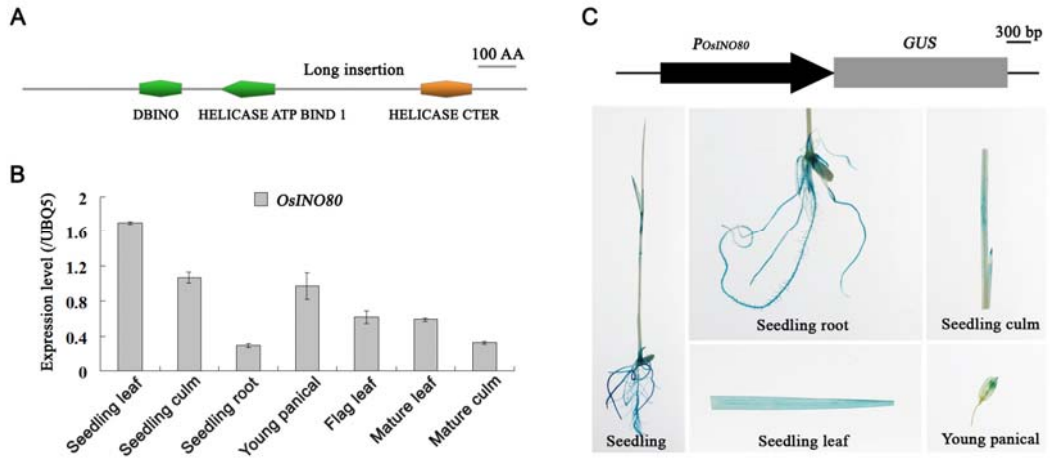

Figure S1. *OsINO80* is broadly expressed throughout the plant.

(A) Protein structure of OsINO80. Polygons indicate domains, as named in PROSITE (http://prosite.expasy.org/).

(B) Expression levels of *OsINO80* determined by quantitative RT-PCR in different tissues: leaf, root, and culm from seedlings, and leaf, flag leaf, culm and young panicles from mature plants. *OsUbiquitin5* served as an internal control. Values shown are means ± SDs of three independent replicates.

(C) Tissue expression pattern analyses of *OsINO80* by histochemical GUS staining in $P_{OsINO80}$*::GUS* transgenic plants. Staining was performed in seedlings and panicles.

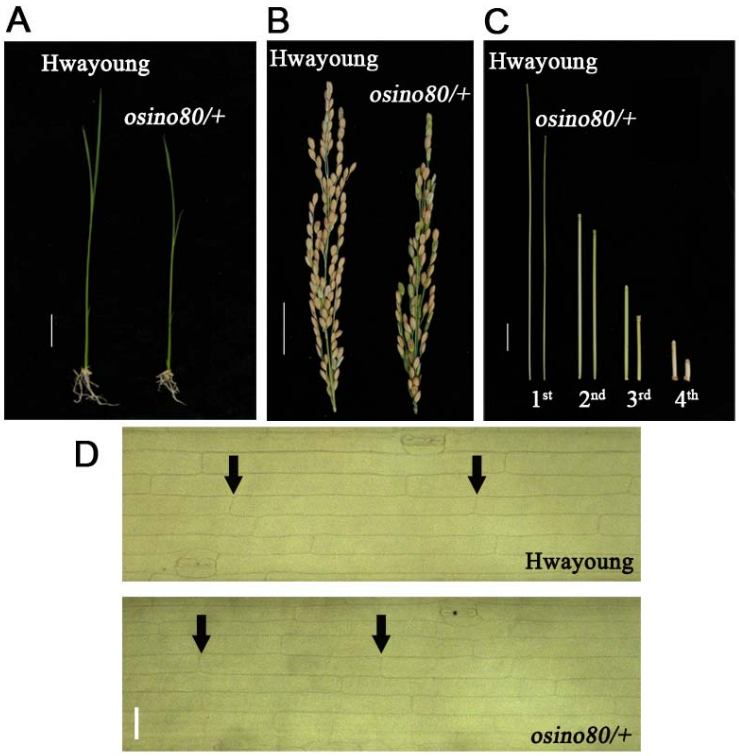

Figure S2. Detailed morphologies of ‘Hwayoung’ and *osino80/+* plants.

(A) Two-week-old seedlings of wild-type ‘Hwayoung’ (left) and *osino80/+* (right) plants. Bar = 3 cm.

(B) First panicles of wild-type ‘Hwayoung’ (left) and *osino80/+* (right) plants. Bar = 3 cm.

(C) Four uppermost internodes of wild-type ‘Hwayoung’ (left) and *osino80/+* (right) plants. Bar = 3 cm.

(D) Cells of the second leaf sheaths in wild-type ‘Hwayoung’ and *osino80/+* plants. Bar = 20 μm. Arrows indicate the cell ends.

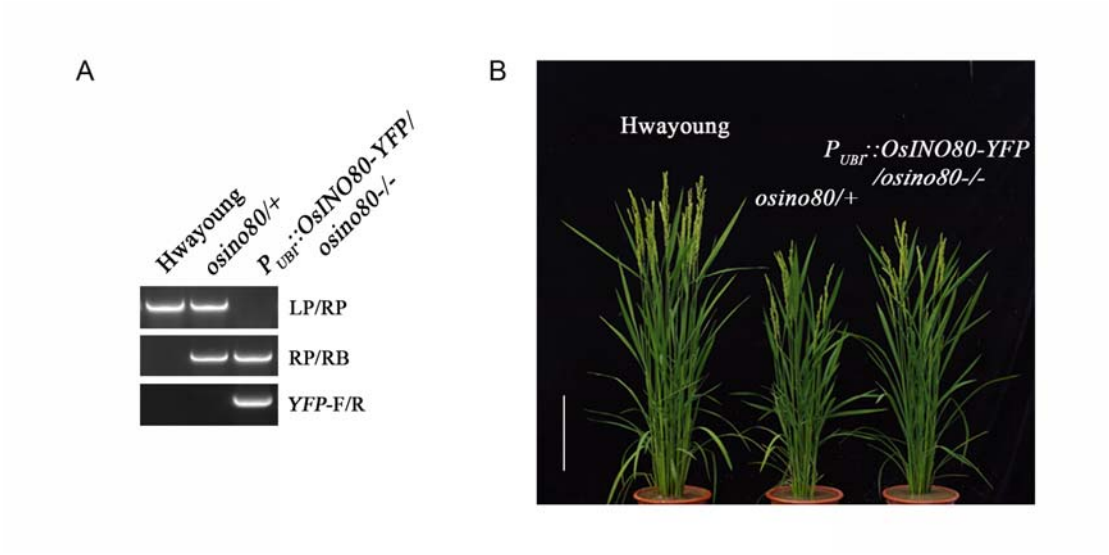

Figure S3. PCR identification and phenotype observation in *P*$_{UBI}$*::OsINO80-YFP*/*osino80*-/-.

(A) PCR amplifications from genomic DNA of the indicated genotypes (top) using the indicated primer pairs (right).

(B) Overall morphologies of the wild-type 'Hwayoung', *osino80/*+, and *P*$_{UBI}$*::OsINO80-YFP*/*osino80*-/-. Bar = 15 cm.

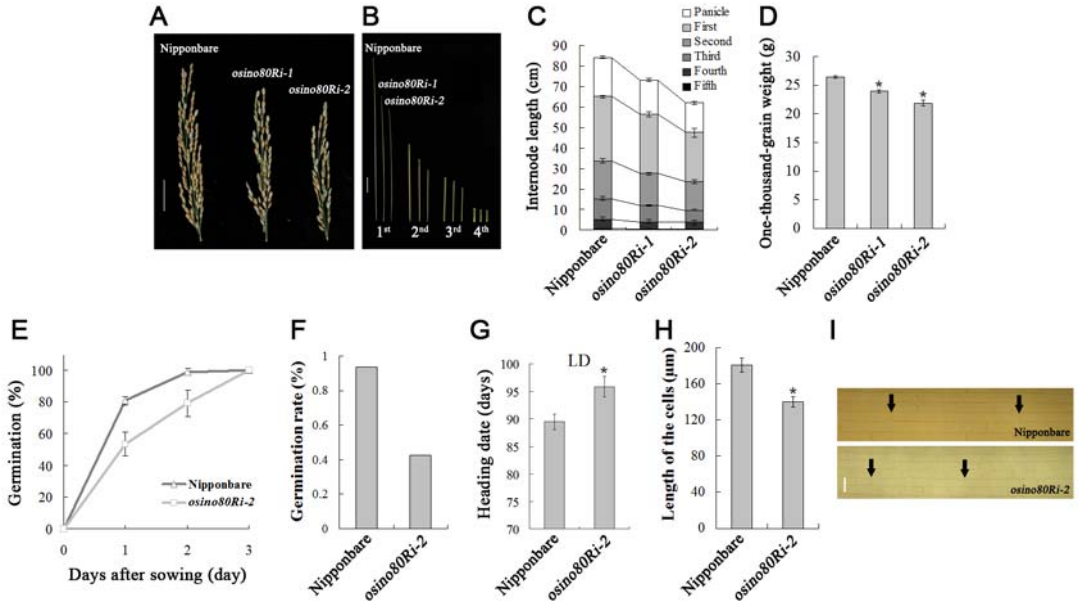

Figure S4. Detailed morphologies of *OsINO80*-knockdown plants by RNA interference.

(A) First panicles of wild-type 'Nipponbare' (left), *osino80Ri-1* (middle), and *osino80Ri-2* (right) plants. Bar = 3 cm. (B) Four uppermost internodes of 'Nipponbare' (left), *osino80Ri-1* (middle), and *osino80Ri-2* (right) plants. Bar = 3 cm. (C) Lengths of panicles and internodes of wild-type 'Nipponbare', *osino80Ri-1,* and *osino80Ri-2* plants. (D) One-thousand-grain weights of seeds from the wild-type 'Nipponbare', *osino80Ri-1*, and *osino80Ri-2* plants. Asterisks indicate statistically significant differences between the indicated genotypes and the wild-type 'Nipponbare' ($P < 0.05$). (E) Seed germination rates in the wild-type 'Nipponbare' and *osino80Ri-2* plants on Murashige and Skoog solid medium. Values shown are means ± SDs (n = 30). (F) Pollen germination rates in the wild-type 'Nipponbare' and *osino80Ri-2* plants. (G) Heading time of the wild-type 'Nipponbare' and *osino80Ri-2* plants grown under LD (Shanghai) conditions. Values shown are means ± SDs (n = 30). Asterisks indicate statistically significant differences between *osino80Ri-2* and the wild-type 'Nipponbare' ($P < 0.05$). (H) Cell lengths in the second leaf sheaths in wild-type 'Nipponbare' and *osino80Ri-2* plants. Asterisks indicate statistically significant differences between *osino80Ri-2* and the wild-type 'Nipponbare' ($P < 0.05$). (I) Cells of the second leaf sheaths in the wild-type 'Nipponbare' and *osino80Ri-2* plants. Bar = 20 μm. Arrows indicates the cell ends.

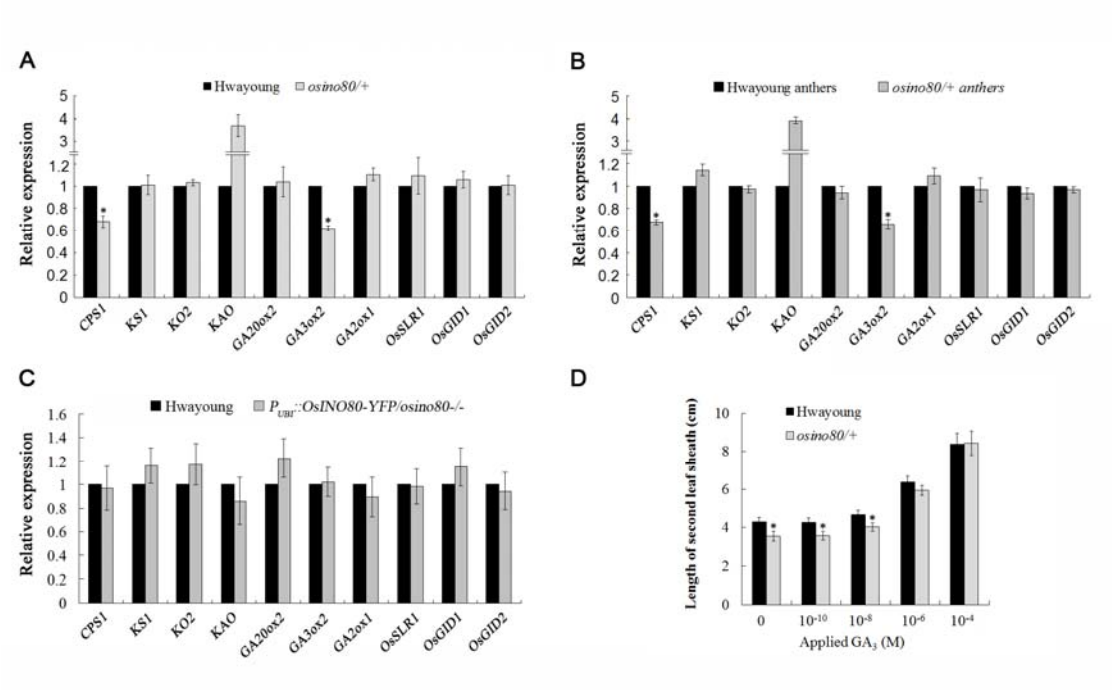

Figure S5. The GA synthesis genes *CPS1* and *GA3ox2* are down-regulated in *osino80/+* and the exogenous GA_3 can rescue the dwarf phenotype of *osino80/+* young seedlings.

(A) Relative expression levels of GA-related genes in the indicated plants. *OsUbiquitin5* served as the internal control, and the fold change relative to the wild-type level is shown. Values shown are means ± SDs from three independent replicates. Asterisks indicate statistically significant differences between the *Osino80/+* and the wild-type ($P < 0.05$). (B) Relative expression levels of GA-related genes in the anthers of wild-type 'Hwayoung' and *osino80/+*. *OsUbiquitin5* served as the internal control, and the fold change relative to the wild-type level is shown. Values shown are means ± SDs from three independent replicates. Asterisks indicate statistically significant differences between the *osino80/+* and the wild-type ($P < 0.05$). (C) Relative expression levels of GA-related genes in the wild-type 'Hwayoung' and *P_{UBI}::OsINO80-YFP/osino80-/-* plants. *OsUbiquitin5* served as the internal control, and the fold change relative to the wild-type level is shown. Values shown are means ± SDs from three independent replicates. (D) Effects of different concentrations of gibberellic acid (GA_3) on the wild-type 'Hwayoung' and *osino80/+*. The lengths of the second leaf sheaths were measured. Values are means ± SDs (n = 20). Asterisks indicate statistically significant differences between *osino80/+* and the wild-type 'Hwayoung' ($P < 0.05$).

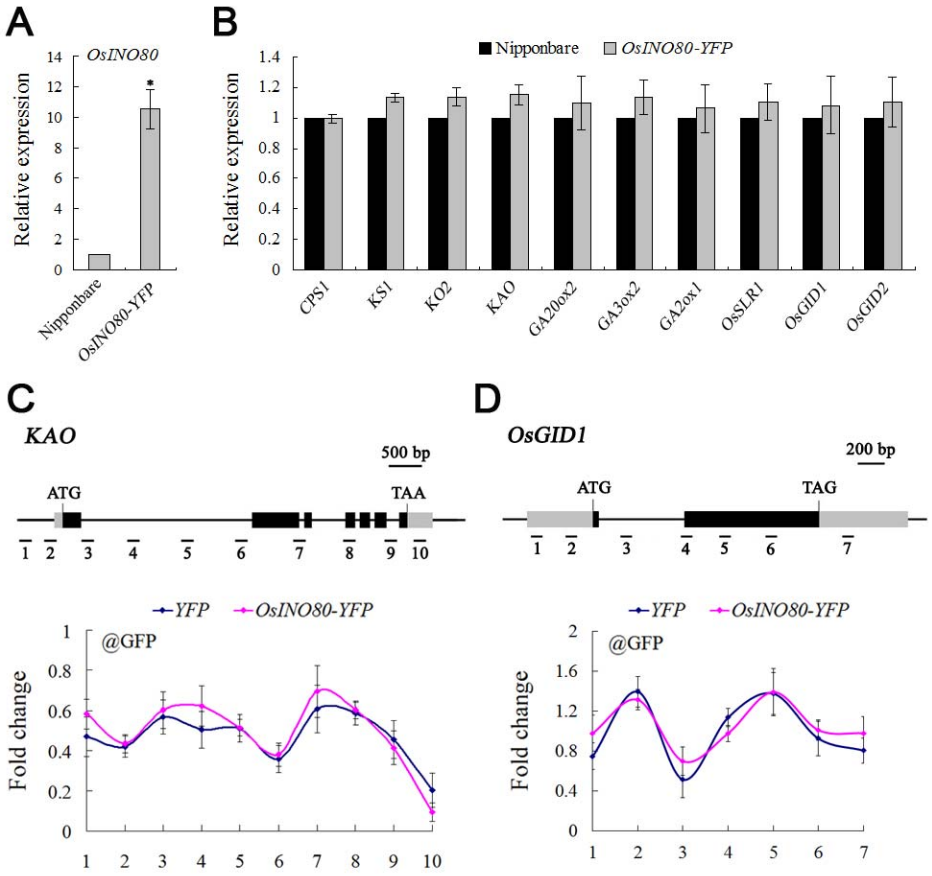

Figure S6. Gene expressions and ChIP analyses in *OsINO80-YFP* plants.

(A,B) Relative expression levels of *OsINO80* (A) and GA-related genes (B) in the indicated plants. *OsUbiquitin5* served as the internal control. Values shown are means ± SDs from three independent replicates. Asterisks indicate statistically significant differences between *OsINO80-YFP* and the wild-type 'Nipponbare' ($P < 0.05$).

(C) Enrichment of OsINO80-YFP at *KAO* chromatin analyzed by ChIP analysis using GFP antibodies. Diagram representing *KAO* gene structure. Bars labeled 1–10 denote regions amplified by PCR. Error bars show standard deviations from three biological replicates.

(D) Enrichment of OsINO80-YFP at *OsGID1* chromatin analyzed by ChIP analysis using GFP antibodies. Diagram representing *OsGID1* gene structure. Bars labeled 1–7 denote regions amplified by PCR. Error bars show standard deviations from three biological replicates.

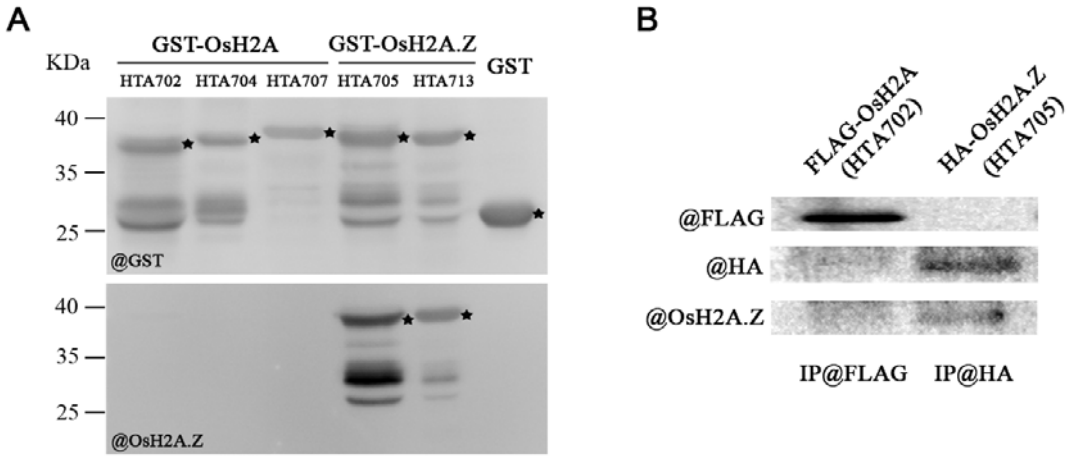

Figure S7. Specificity tests of the OsH2A.Z antibody *in vitro* and *in vivo*.

(A) Purified GST-fused OsH2A or OsH2A.Z analyzed by western blotting using GST antibodies (top panel) or OsH2A.Z antibodies (bottom panel).

(B) Immunoprecipitated protein extracts from rice mesophyll protoplasts expressing *FLAG-OsH2A* and *HA-OsH2A.Z* analyzed by western blot using the antibodies against FLAG or HA.

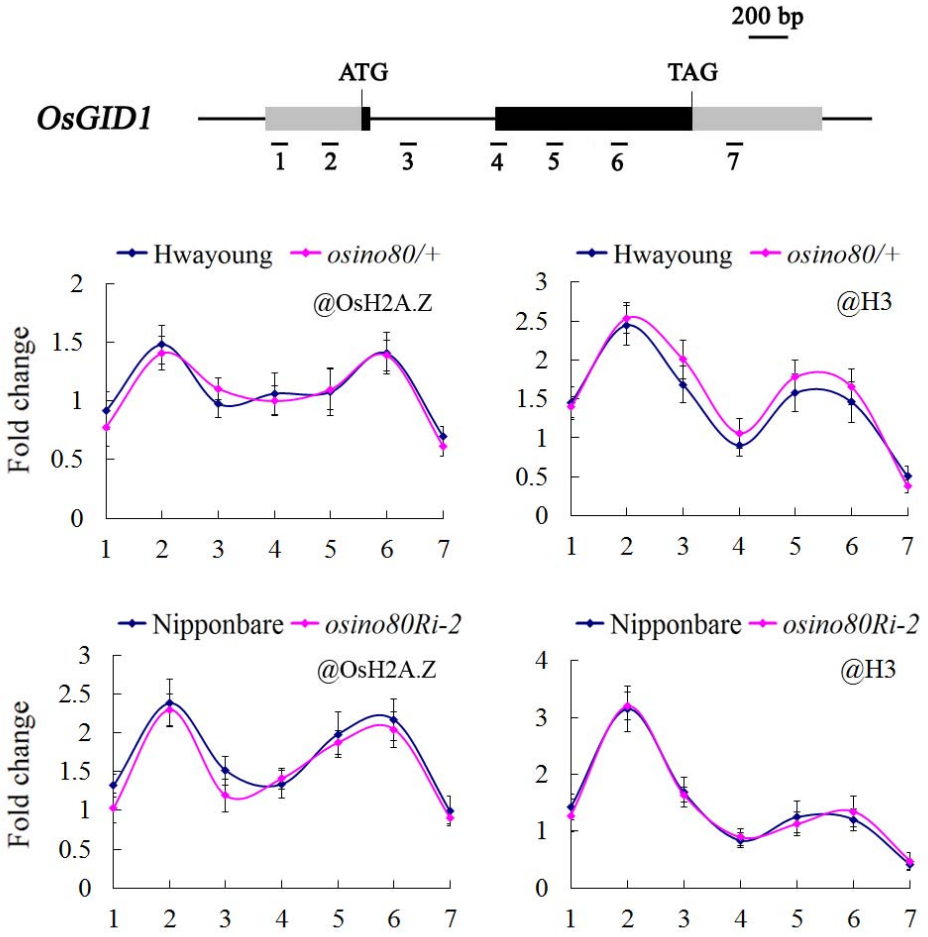

Figure S8. ChIP analyses using antibodies against OsH2A.Z or H3 at *OsGID1* chromatin in indicated genotypes.

Diagram representing the *OsGID1* gene structure. Bars labeled 1–7 denote regions amplified by PCR. Error bars show standard deviations from three biological replicates.

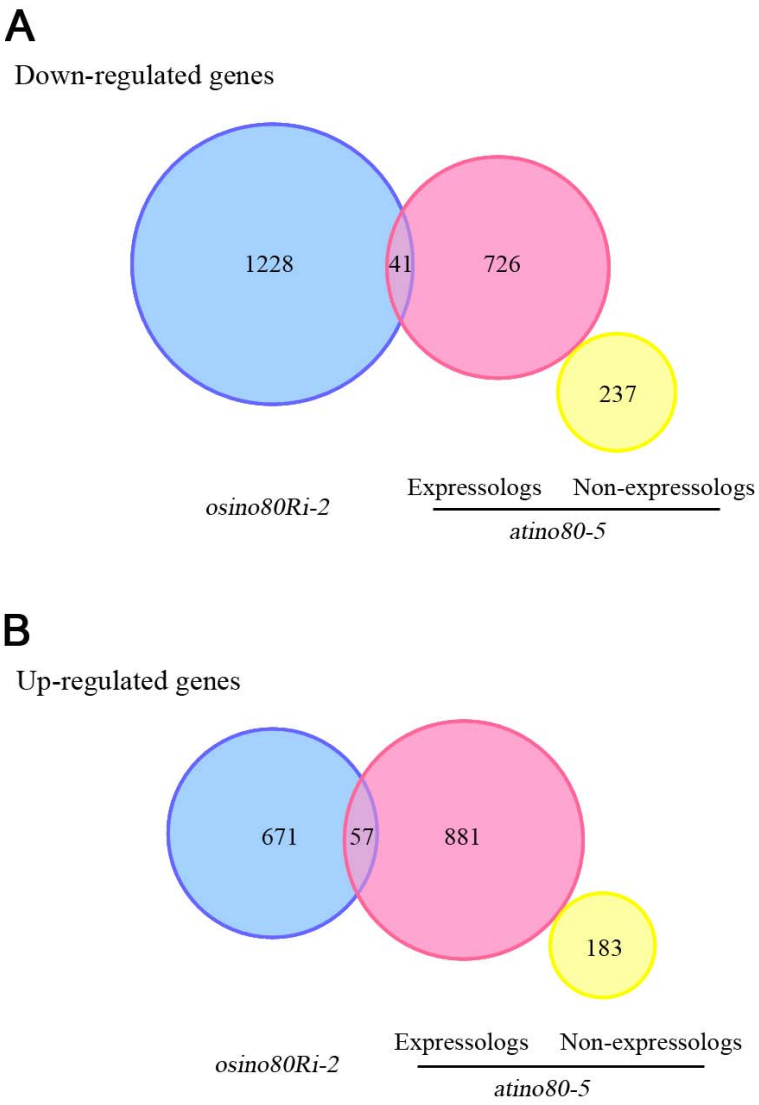

Figure S9. Comparison of the transcriptome profiles between rice *osino80Ri-2* and Arabidopsis *atino80-5* mutants.

Venn diagrams show the number of genes mis-regulated.

Table S1. Genes down- or up-regulated by more than twofold in *osino80Ri-2* compared with those in the wild-type plants.

Table S2. Transcription levels of *OsINO80* and GA-related genes in the RNA-seq data of the wild-type and *osino80Ri-2* plants.

Table S3. Primers used in the study.

Table S4. Mapping information of RNA-seq data.